

AD _____

GRANT NUMBER: DAMD17-94-J-4474

TITLE: Sequence-Specific and Synergistic Binding of Drugs to DNA

PRINCIPAL INVESTIGATOR: Fu-Ming Chen, Ph.D.

CONTRACTING ORGANIZATION: Tennessee State University
Nashville, Tennessee 37209-1561

REPORT DATE: October 1995

TYPE OF REPORT: Annual

PREPARED FOR: U.S. Army Medical Research and Materiel Command
Fort Detrick, Maryland 21702-5012

DISTRIBUTION STATEMENT: Approved for public release;
distribution unlimited

The views, opinions and/or findings contained in this report are those of the author(s) and should not be construed as an official Department of the Army position, policy or decision unless so designated by other documentation.

19960410 006

FILE QUALITY INSPECTED 1

REPORT DOCUMENTATION PAGE			Form Approved OMB No. 0704-0188	
Public reporting burden for this collection of information is estimated to average 1 hour per response, including the time for reviewing instructions, searching existing data sources, gathering and maintaining the data needed, and completing and reviewing the collection of information. Send comments regarding this burden estimate or any other aspect of this collection of information, including suggestions for reducing this burden, to Washington Headquarters Services, Directorate for Information Operations and Reports, 1215 Jefferson Davis Highway, Suite 1204, Arlington, VA 22202-4302, and to the Office of Management and Budget, Paperwork Reduction Project (0704-0188), Washington, DC 20503.				
1. AGENCY USE ONLY (Leave blank)		2. REPORT DATE October 1995		3. REPORT TYPE AND DATES COVERED Annual 23 Sep 94 - 22 Sep 95
4. TITLE AND SUBTITLE Sequence-Specific and Synergistic Binding of Drugs to DNA			5. FUNDING NUMBERS DAMD17-94-J-4474	
6. AUTHOR(S) Fu-Ming Chen, Ph.D.				
7. PERFORMING ORGANIZATION NAME(S) AND ADDRESS(ES) Tennessee State University Nashville, Tennessee 37209-1561			8. PERFORMING ORGANIZATION REPORT NUMBER	
9. SPONSORING/MONITORING AGENCY NAME(S) AND ADDRESS(ES) U.S. Army Medical Research and Materiel Command Fort Detrick, Maryland 21702-5012			10. SPONSORING/MONITORING AGENCY REPORT NUMBER	
11. SUPPLEMENTARY NOTES				
12a. DISTRIBUTION/AVAILABILITY STATEMENT Approved for public release; distribution unlimited			12b. DISTRIBUTION CODE	
13. ABSTRACT (Maximum 200 words) We had proposed to study the sequence specific binding and synergistic effect of three drugs having distinctly different binding modes: actinomycin D (ACTD), a guanine specific intercalator; chromomycin A ₃ , a guanine specific minor groove binder; and distamycin A, an A•T specific groove binder. To investigate the possible synergistic effects of drugs on DNA binding, it is essential that binding characteristics of each individual drug such as binding affinities, sequence specificities, and kinetic behaviors be well understood. During the past year, our laboratory has focused mainly on the detailed studies of ACTD. Comparative studies with dodecamers of the form d(AAAA-XGCX-TTTT) suggest that ACTD binds strongly to a 5'GC3' site with flanking T / T or C / C mismatches but weakly to that with G / G or A / A mismatches. In our binding studies with hairpins, it was found that this drug binds strongly to GpC- as well as some non-GpC-containing stems. We have also investigated the origin of its strong binding to a non-GC-containing octamer d(CGTCGACG) and concluded that it most likely is the consequence of end-stacking. During this period, we have also uncovered an interesting phenomenon of K ⁺ -induced supramolecular assembly of G-quadruplexes in d(CGG) ₄ which is inhibited by ACTD binding.				
14. SUBJECT TERMS DNA, Binding, Intercalation, Synergistic effect. Breast Cancer			15. NUMBER OF PAGES 47	
			16. PRICE CODE	
17. SECURITY CLASSIFICATION OF REPORT Unclassified	18. SECURITY CLASSIFICATION OF THIS PAGE Unclassified	19. SECURITY CLASSIFICATION OF ABSTRACT Unclassified	20. LIMITATION OF ABSTRACT Unlimited	

GENERAL INSTRUCTIONS FOR COMPLETING SF 298

The Report Documentation Page (RDP) is used in announcing and cataloging reports. It is important that this information be consistent with the rest of the report, particularly the cover and title page. Instructions for filling in each block of the form follow. It is important to **stay within the lines** to meet **optical scanning requirements**.

Block 1. Agency Use Only (Leave blank).

Block 2. Report Date. Full publication date including day, month, and year, if available (e.g. 1 Jan 88). Must cite at least the year.

Block 3. Type of Report and Dates Covered. State whether report is interim, final, etc. If applicable, enter inclusive report dates (e.g. 10 Jun 87 - 30 Jun 88).

Block 4. Title and Subtitle. A title is taken from the part of the report that provides the most meaningful and complete information. When a report is prepared in more than one volume, repeat the primary title, add volume number, and include subtitle for the specific volume. On classified documents enter the title classification in parentheses.

Block 5. Funding Numbers. To include contract and grant numbers; may include program element number(s), project number(s), task number(s), and work unit number(s). Use the following labels:

C - Contract	PR - Project
G - Grant	TA - Task
PE - Program Element	WU - Work Unit Accession No.

Block 6. Author(s). Name(s) of person(s) responsible for writing the report, performing the research, or credited with the content of the report. If editor or compiler, this should follow the name(s).

Block 7. Performing Organization Name(s) and Address(es). Self-explanatory.

Block 8. Performing Organization Report Number. Enter the unique alphanumeric report number(s) assigned by the organization performing the report.

Block 9. Sponsoring/Monitoring Agency Name(s) and Address(es). Self-explanatory.

Block 10. Sponsoring/Monitoring Agency Report Number. (If known)

Block 11. Supplementary Notes. Enter information not included elsewhere such as: Prepared in cooperation with...; Trans. of...; To be published in.... When a report is revised, include a statement whether the new report supersedes or supplements the older report.

Block 12a. Distribution/Availability Statement. Denotes public availability or limitations. Cite any availability to the public. Enter additional limitations or special markings in all capitals (e.g. NOFORN, REL, ITAR).

DOD - See DoDD 5230.24, "Distribution Statements on Technical Documents."

DOE - See authorities.

NASA - See Handbook NHB 2200.2.

NTIS - Leave blank.

Block 12b. Distribution Code.

DOD - Leave blank.

DOE - Enter DOE distribution categories from the Standard Distribution for Unclassified Scientific and Technical Reports.

NASA - Leave blank.

NTIS - Leave blank.

Block 13. Abstract. Include a brief (*Maximum 200 words*) factual summary of the most significant information contained in the report.

Block 14. Subject Terms. Keywords or phrases identifying major subjects in the report.

Block 15. Number of Pages. Enter the total number of pages.

Block 16. Price Code. Enter appropriate price code (*NTIS only*).

Blocks 17. - 19. Security Classifications. Self-explanatory. Enter U.S. Security Classification in accordance with U.S. Security Regulations (i.e., UNCLASSIFIED). If form contains classified information, stamp classification on the top and bottom of the page.

Block 20. Limitation of Abstract. This block must be completed to assign a limitation to the abstract. Enter either UL (unlimited) or SAR (same as report). An entry in this block is necessary if the abstract is to be limited. If blank, the abstract is assumed to be unlimited.

FOREWORD

Opinions, interpretations, conclusions and recommendations are those of the author and are not necessarily endorsed by the US Army.

N/A Where copyrighted material is quoted, permission has been obtained to use such material.

N/A Where material from documents designated for limited distribution is quoted, permission has been obtained to use the material.

N/A Citations of commercial organizations and trade names in this report do not constitute an official Department of Army endorsement or approval of the products or services of these organizations.

N/A In conducting research using animals, the investigator(s) adhered to the "Guide for the Care and Use of Laboratory Animals," prepared by the Committee on Care and Use of Laboratory Animals of the Institute of Laboratory Resources, National Research Council (NIH Publication No. 86-23, Revised 1985).

N/A For the protection of human subjects, the investigator(s) adhered to policies of applicable Federal Law 45 CFR 46.

N/A In conducting research utilizing recombinant DNA technology, the investigator(s) adhered to current guidelines promulgated by the National Institutes of Health.

N/A In the conduct of research utilizing recombinant DNA, the investigator(s) adhered to the NIH Guidelines for Research Involving Recombinant DNA Molecules.

N/A In the conduct of research involving hazardous organisms, the investigator(s) adhered to the CDC-NIH Guide for Biosafety in Microbiological and Biomedical Laboratories.

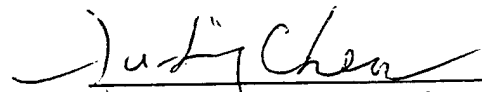
 10-17-95
PI - Signature Date

TABLE OF CONTENTS

	PAGE
FRONT COVER	
SF 298 REPORT DOCUMENTATION PAGE	1
FOREWORD	2
TABLE OF CONTENTS	3
INTRODUCTION	4
BODY	6
CONCLUSIONS	22
REFERENCES	22
TABLES	24-29
FIGURE LEGENDS	30-31

INTRODUCTION

Combination chemotherapy is one of the important strategies in cancer treatments. This is based on the observation that administering certain drugs together is more effective than giving individual drugs separately. Although the reason for such an effect is not understood, it may be related to the synergistic effect of their binding to macromolecules. Consequently, studies on the interplay among drugs capable of binding to different regions of DNA will be of considerable interest. Understanding the synergism of drugs at the molecular level may have important implication for designing more effective chemotherapeutic strategies in breast cancer treatments. Our proposal focuses on sequence specific binding and synergistic effect of three drugs having distinctly different binding modes: actinomycin D (ACTD), a guanine specific intercalator; chromomycin A₃ (CHR), a guanine specific minor groove binder; and distamycin A (DST), an A•T specific groove binder. In order to investigate the possible synergistic effects of drugs on DNA binding, it is essential that binding characteristics of each individual drug such as binding affinities, sequence specificities, and kinetic behaviors be thoroughly elucidated.

During the past year, we have focused on the detailed studies of actinomycin D. This resulted from the fact that prior to the awarding of the grant, my laboratory was engaged in sequence specific binding studies of actinomycin D to some unusual DNA conformations. Since the initial results coming out of these studies were quite interesting and requiring further experimentations, we decided to continue these lines of investigation. This action deviates somewhat from the originally proposed timeline and scope but can be justified on the ground that sequence specific binding study of actinomycin D is part of the proposed SOW, albeit more related to Task#3 than to Task#1. It was the oversight on the part of the PI not to have asked for the prior approval for taking such an action. The PI is hereby requesting the approval for the following revised SOW and timeline:

Task 1: Sequence specific binding studies of actinomycin D to GC- and non-GC-containing sequences of usual and unusual DNA conformations. The unusual DNA conformations to be studied include hairpins, duplex with base mismatches and G-quadruplexes. Months 1-12.

Task 2: Sequence specific binding studies of chromomycin A₃ at the self- and non-self-complementary tetranucleotide level. Months 13-24.

Task 3: Sequence specific binding studies of distamycin at the self- and non-self-complementary tetranucleotide level. Months 25-36.

Task 4: Studies on synergistic effects of drugs. Months 37-48.

Actinomycin D (ACTD) is an antitumor antibiotic that contains a 2-aminophenoxazin-3-one chromophore and two cyclic pentapeptide lactones. Its DNA binding mode and base sequence specificity have been well characterized by X-ray crystallography (Sobell & Jain, 1972; Takusagawa et al., 1982; Kamitori & Takusagawa, 1992), footprinting (Lane et al., 1983; Scamrov & Beabealashvilli, 1983; Van Dyke & Dervan, 1983; Van Dyke et al., 1983; Fox & Waring, 1984; White & Phillips, 1989; Reh fuss et al., 1990; Goodisman et al., 1992; Goodisman & Dabrowiak, 1992), hydrodynamic (Muller & Crothers, 1968), and spectroscopic (Krug h, 1972; Patel, 1974; Krug h et al., 1977; Brown et al., 1984; Scott et al., 1988ab; Zhou et al., 1989; Brown et al., 1994) measurements. The most recent crystallographic study with d(GAAGCTTC)₂ has largely confirmed the earlier proposed intercalative model and provided additional structural details (Kamitori & Takusagawa, 1994). The complex is formed by phenoxazinone chromophore intercalating into the 5'GC3' sequence from the minor groove, with the two cyclic pentapeptide rings resting on both sides of the minor groove and covering four base pairs of DNA. Four threonine-guanine hydrogen bonds and two additional hydrogen bonds between the N2 amino group of phenoxazone and the DNA backbone are formed. The preference of this drug for the 5'-GpC-3' step is, thus, the consequence of these threonine-guanine hydrogen bond formations. These essential drug-DNA hydrogen bonds are protected by the cyclic pentapeptides which effectively shield them from solvent exposure.

The size of the four base-paired binding site suggests that the binding characteristics of ACTD to the GC site may be affected by the flanking adjacent base pairs. Indeed, studies with self- as well as non-self-complementary -XGCMY-containing decamers (Chen, 1988a,b; 1992) have revealed that the binding affinity and dissociation kinetics of this drug are greatly affected by the nature of the X and Y bases. For example, ACTD binds strongly to and dissociates very slowly from the -TGCA- site, whereas it binds weakly and dissociates very rapidly from the -GGCC- sequence. Similar adjacent base-pair effects had also been observed by others (Aivasashvilli & Beabealashvilli, 1983; Rill *et al.*, 1989).

We have now extended such studies to include adjacent base-mismatches. It is known that DNA base-pair mismatches can sometimes serve as initiators or intermediates in a mutagenic pathway and they may be introduced during replication (Modrich, 1987), recombination (Akiyama et al., 1989), or other chemical events. These sites can also serve as preferential targets for drugs or carcinogens. Effects of base pair mismatches on DNA structures (Hunter, 1992) and their ligand interactions are, thus, of considerable interest, as they may have relevance in DNA repair, transcription, replication, and activation of damaged genes. A logical extension to our earlier studies on the adjacent base pair effect on the ACTD binding to a GC site would be to investigate the effect of the flanking base mismatches on the affinity and kinetic behaviors of this preferred sequence. Part of this report describes results of such studies but focuses only on ACTD binding and kinetic investigations on GC sites flanked by homobase mismatches. Comparative studies using dodecamers containing self-complementary -XGCMY- and non-self-complementary -XGCMX- sequences were carried out to accomplish our objectives.

Despite the well established GC sequence specificity of ACTD, there have been reports to indicate that ACTD can also bind strongly to some non-GC sequences (Synder,

et al., 1989; Rill, et al., 1989; Bailey, et al., 1994) as well as to some single-stranded DNA (Wadkins & Jovin; 1991). In particular, calorimetric studies by Snyder et al. (1989) had led to the conclusion that ACTD binds cooperatively to octamer d(5'CGTCGACG3') with a binding constant higher than 10^7 M^{-1} and a 2:1 drug to duplex ratio. It is important to understand the nature of such a strong binding and to delineate the origin of its high cooperativity. Since it has been suggested by Snyder, et al. (1989) that the mode of ACTD binding to d(CGTCGACG) is distinct from its classic mode of binding to GpC sequence, it will be of value to see if this is in fact the case. To this end, the possibility that the cooperative and strong ACTD binding of this oligomer to be the consequence of the drug molecules stacking at the ends of the DNA duplex, in conformity with the classic binding preference, was investigated. The results of these experiments and their significance will also be presented and discussed in this report.

Our laboratory has also been interested in unusual DNA conformations and their interactions with drugs. In the past, our works touched on Z-form, triplex, and G-quadruplex DNAs. During the past year, our ACTD binding studies have also been extended to its binding to hairpins with stems containing GC as well as non-GC sequences. Although extensive works on various aspects of ACTD binding to DNA had been made in the past, few studies were carried out on its binding to the hairpin form of DNA. In an effort to understand the binding to such motifs, studies have been carried out with decamers which form exclusively hairpin conformations. Of particular interest is the effect of the GC site location in the stem on the binding affinity and kinetic behavior of ACTD-DNA interactions. Binding of ACTD to hairpins without GC containing stem has also been addressed.

Some efforts have also been invested in studying the K^+ -induced supramolecular self-assembly of CGG trinucleotides repeats, an interesting phenomenon which was recently uncovered in our laboratory (Chen, 1995). The interest in this phenomenon stems from the fact that fragile X syndrome is the most common cause of inherited mental retardation. Individuals affected by this disorder have an X chromosome in which the tip of its long arm is attached by only a slender thread of DNA. A gene designated as FMR-1 contains about 60 or fewer tandem repeats of CGG trinucleotide sequence in normal individuals. In sick individuals, however, the tandem repeat region is dramatically amplified (Sutherland & Richards, 1994). Recently, amplifications of trinucleotide repeats have also been shown to be associated with several other disorders, including Kennedy and Huntington diseases. Although the mechanism of this unusual trinucleotide amplification is still unknown, it would not be surprising if there were structural bases for such remarkable amplifications. ACTD binding to some trinucleotide repeats has also been investigated.

Since the results on the ACTD binding to unusual DNA conformations are currently in the process of being organized, only brief summaries without detailed expositions will be made in this report.

BODY

ACTD Binding to 5'GC3' Sites Flanked by Homo-base Mismatches.

Rationale for the Choice of Oligomers. Dodecamers of the form

d(AAAA-XGCX-TTTT), where X = A, T, G, or C, were chosen for this study. Except for the X base, this sequence is self-complementary and contains a single GC site at the center. If such a dodecamer forms a dimeric duplex, the central region will consist of a 5'GC3' step with flanking X/X mismatches. Such a sequence can, however, also fold back on itself to form a hairpin consisting of a 4-base-paired stem and a 4-base loop. The presence of mismatches will significantly destabilize the dimeric duplex and facilitate the hairpin formation. The hairpin conformation would, however, place the GC sequence at the loop region with only A•T base pairings in the duplex stem, consequently, would be expected to greatly diminish its ACTD binding affinity. Thus, despite the anticipated significant or even dominant presence of hairpin conformations in solutions, it follows that if ACTD binds strongly to a duplex GC sequence with flanking base mismatches, it will further shift the equilibrium to favor the dimeric duplex for additional binding to result in a predominance of drug complexation with dimeric duplexes. Comparative studies of these sequences will, consequently, yield the relative binding order of these mismatched sequences and parallel studies with the corresponding self-complementary dodecamers containing the -XGCY- sequences will provide comparison with the known strong binding sites. The additional rationale for carrying out studies on self-complementary dodecamers is to further investigate the effects of adjacent base pairs and flanking sequences on the ACTD binding characteristics at the GC site and to compare with our earlier results using decamers of the form d(ATA-XGCY-TAT) (Chen, 1988b, 1992).

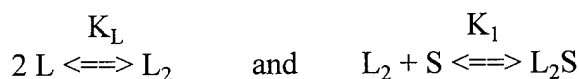
Electrophoretic Mobility Patterns of Oligomers and Their Drug Complexes. To substantiate our rationalization on the oligomeric choice, electrophoretic measurements were made with oligomers in the presence and in the absence of ACTD (results not shown). Comparison of electrophoretic mobility patterns at 4 °C of selective self-complementary and mismatched dodecamers and in the presence of ACTD indicates that the self-complementary dodecamers are dominated by bands which can reasonably be assigned as those of dimeric duplexes. A slight retardation of the electrophoretic mobility of the dimeric duplex band in the presence of ACTD can readily be discerned, suggesting strong binding to the self-complementary -TGCA- and -AGCT- sequences. In contrast, dodecamers with X/X mismatches are dominated by a considerably faster-moving band even at this low temperature, indicating the predominance of monomeric hairpin conformations for the mismatched oligomers. Despite the predominance of the hairpin species, however, the retarded electrophoretic bands due to ACTD binding to oligomers with T/T or C/C mismatches exhibit mobilities which are identical to those of dimeric duplex-ACTD bands of the self-complementary counterparts. Although the presence of ACTD had largely abolished the hairpin band for the dodecamer with T/T mismatches, significant intensity of this band is retained for that of C/C mismatches, suggesting higher ACTD binding affinity and/or slower dissociation kinetics for the dodecamer with T/T than that of C/C mismatches. Similar measurements with dodecamers of A/A and G/G mismatches failed to reveal any significant differences between the electrophoretic mobility patterns in the absence and in the presence of ACTD. These results support the notion that the presence of ACTD can facilitate the dimeric duplex formation for some mismatched dodecamers via binding to the GC site

and further suggest that the binding affinities for the flanking pyr/pyr mismatches are considerably higher than those with pur/pur mismatches.

Absorbance Spectral Evidence of Strong ACTD Binding for Dodecamers with T/T or C/C Mismatches. Absorbance spectral titrations were carried out to obtain more quantitative binding parameters. DNA binding to ACTD results in absorbance intensity depression and enhancement at the 427 and 480 nm regions, respectively. Thus, a qualitative ranking of relative binding affinity of ACTD with different sequences can be achieved by simply comparing the intensity alterations near these regions in the presence of various oligomers of the same [nucleotide] / [drug] (P/D) ratio. Absorption difference spectra of 5 μ M ACTD in the presence (P/D = 40) and in the absence of DNA are compared in Fig. 1 for self-complementary (panel A) and mismatched (panel B) dodecamers. Consistent with our earlier findings with decamers (Chen, 1988b), ACTD affinity for the -GGCC- sequence is considerably weaker than the other three self-complementary -XGCRY- sequences which exhibit intensity alterations of comparable magnitude. Interestingly, the absorbance changes induced by ACTD binding to dodecamers containing C/C and T/T mismatches are sizable and are in fact comparable to the self-complementary counterparts in terms of magnitude as well as spectral characteristics (compare panels A and B). Such intensity comparisons amongst dodecamers containing a GC sequence with flanking homo-base mismatches (panel B) further suggest a qualitative ranking on the binding order of: T/T > C/C > G/G > A/A for the flanking mismatched pairs.

Oligomers with T/T and C/C Mismatches Exhibit Unusual Curvatures in the Scatchard Plots. To obtain more quantitative binding parameters, the titration data at fixed wavelengths were converted to Scatchard plots. Results of T/T and C/C-mismatched dodecamers along with three self-complementary oligomers are compared in Fig. 2. It is immediately apparent that in contrast to the self-complementary oligomers, the plots for the two mismatched dodecamers exhibit unusual curvatures as if the initial low P/D data points were emanating from the origin which at higher P/D revert to a 'normal' linear plot. The binding affinities of these two mismatched oligomers, as revealed by the slopes at the high P/D regions, are comparable and are seen to be slightly weaker than -TGCA- but somewhat stronger than those of self-complementary -CGCG- and -AGCT- sequences. In contrast to the binding densities of around 0.05 (or 1 drug molecule per duplex as to be expected) for the self-complementary sequences, the two mismatched dodecamers extrapolated to approximately 0.035 (or 0.8 drug molecules per duplex). The approximate binding parameters as extracted via linear least-squares fits to the higher P/D data points are summarized in Table 1. The lower binding densities of less than one drug molecule per duplex, as exhibited by the mismatched oligomers, are consistent with the significant presence of non-binding hairpin conformations in these mismatched oligomers.

Fitting the Binding Isotherms with a Binding Model. To investigate the possibility of obtaining more reliable binding constants via model fitting for those isotherms which exhibit Scatchard plots of unusual curvatures, the following model is assumed: that the monomeric hairpin (L) is in dynamic equilibrium with the dimeric duplex (L_2) but only the dimeric duplex form binds with the drug (S) to form a 1:1 drug-DNA complex (L_2S):



By means of equations for the mass balances of DNA (in strand) and ACTD, the following equations can be derived:

$$2 (S_t - S)(1 + K_1) + [K_1 S (S_t - S) / K_L]^{1/2} - L_t K_1 S = 0 \quad (1)$$

$$L_2 = (S_t - S) / K_1 S \quad (2)$$

$$A = \epsilon_S S + \epsilon_1 S K_1 L_2 \quad (3)$$

where ϵ_S and ϵ_1 are extinction coefficients of free (S) and bound drugs, respectively, and S_t and L_t are respective total drug and DNA strand concentrations. A is the observed absorbance at a given wavelength. For simplicity, brackets were omitted in the concentration expressions. Non-linear least squares fits of the experimental binding isotherms with these equations can be seen to be excellent (Fig. 3). The apparent good fits at the low P/D region, where the Scatchard plots exhibit unusual curvatures, is particularly gratifying. K_1 of 8.9 and 7.4 μM^{-1} and K_L of 0.13 and 0.07 μM^{-1} were found for the T/T and C/C mismatched oligomers, respectively, which are seen to be in general agreement with those estimated via Scatchard plots. The plausibility of the assumed model is strengthened by the extracted K_L of $\ll 1$, in agreement with the predominance of the hairpin species in solutions for the oligomers with C/C and T/T mismatches.

CD Spectral Evidence of ACTD Binding. The effect of ACTD binding to a DNA duplex on the CD spectral characteristics is to induce sizable positive and negative CD intensities at the 293 and 255 nm regions, respectively. Thus, qualitative ACTD binding affinities for these oligomers can also be obtained via difference CD (ACTD/DNA - DNA) spectral comparison. CD difference spectra of four mismatched dodecamers are compared in Fig. 4. It is evident that dodecamers with T/T and C/C mismatches exhibit larger CD difference spectra than those of G/G and A/A mismatches and are comparable to those of the self-complementary counterparts (not shown). The CD results are, thus, consistent with the relative binding order established via absorbance measurements.

ACTD Dissociates Slowly from d(AAAA-TGCT-TTTT). Despite the comparable ACTD binding affinities exhibited by the T/T and C/C mismatched dodecamers, their kinetic behaviors are distinctly different. The non-stopped-flow measurable association and dissociation kinetic traces were analysed by single exponential least-squares fits and the results are summarized in Table 2. The ACTD association rates do not appear to differ greatly among the self-complementary, the T/T, and the C/C mismatched dodecamers. The oligomers with -AGCT- and T/T mismatches exhibit nearly identical association rates which are 2-3 times slower than dodecamers with -TGCA-, -CGCG-, and C/C mismatches. In contrast, the dissociation kinetics are more varied as can be seen in Fig. 5. For example, the T/T-mismatched dodecamer exhibits an order of magnitude slower SDS-induced ACTD dissociation rate than that of the C/C mismatched counterpart. It is interesting and also somewhat surprising that the dissociation rate of the T/T mismatches is in fact comparable to the -TGCA- and -AGCT-containing self-complementary

dodecamers but is considerably slower than the self-complementary -CGCG- dodecamer. It should be mentioned in passing that a single-exponential fit to the association kinetic trace of oligomer with T/T or C/C mismatches is somewhat poor and requires a 2-exponential fit with the apparent presence of a slow component of significant contribution.

Effects of ACTD Binding on the Melting Temperatures of Oligomers. Thermal denaturation profiles with 275-nm monitoring for 40 μ M DNA solutions in the absence and in the presence of ACTD were measured to investigate the effect of ACTD binding on the thermal stabilities of these duplexes. The results are included in Table 1. Due to the destabilization of the duplex form and multi-conformational states of these mismatched oligomers, these DNAs in the absence of ACTD exhibit broad and diffuse melting profiles (not shown). The melting temperatures of the dimeric duplexes were estimated to be below 10 °C from measurements with higher DNA concentrations. In the presence of 5 μ M ACTD, however, the melting profiles for the T/T, C/C, and G/G-mismatched dodecamers exhibit highly cooperative transitions near 33, 28, and 20 °C, respectively. No apparent alteration on the melting profile was observed for the A/A-mismatched oligomer. These results are to be compared with the melting temperature increases of 9 to 14 °C as exhibited by the strong binding self-complementary -XGCV-sequences. Thermal denaturation experiments via absorbance monitoring at 427 nm for the drug release were also made and the results (not shown) are in agreement with those of 275 nm monitoring. The melting results, thus, also support the relative binding order established via spectral measurements.

Comparison with the Fluorescence Results of 7-Amino-Actinomycin D (7-AM-ACTD). Although ACTD is only weakly fluorescent, its 7-amino derivative is highly so. Despite the presence of an amino group at the 7 position, its DNA binding mode has been shown to be similar to that of its parent ACTD (Chiao et al., 1979). It is, thus, of interest to corroborate the ACTD results with those of this derivative via fluorescence measurements. The fluorescence emission difference spectra for the strong binding self-complementary -XGCV-containing dodecamers with 560 nm excitation consist of a strong emission maximum at 650 nm and a shoulder near 615 nm, suggesting fluorescence enhancements near these two wavelength regions when 7-AM-ACTD binds to these DNA. The much weaker binding of the -GGCC- sequence is again apparent via the negligible intensity enhancement (not shown). Interestingly, the fluorescence intensity induced by binding to the GC sequence with C/C mismatches is considerably higher than that with T/T mismatches which in turn is somewhat higher than that of the self-complementary -TGCA- sequence. In contrast, the intensities for dodecamers with G/G and A/A mismatches are considerably smaller (see Fig. 6). The similar spectral characteristics support the notion that the mode of binding at the GC site with flanking T/T or C/C mismatches are very similar to those of strong binding self-complementary -TGCA- sequences.

Kinetic measurements were also made by exciting the molecules with 560 nm light and monitoring emission at 650 nm for the association and at 600 nm for the SDS-induced dissociation of 7-AM-ACTD. Results of single exponential fits on these data are compared in Table 3. These results support our absorbance measurements indicating that

the dodecamer with T/T mismatches flanking a GC sequence exhibits a much slower dissociation rate than that with C/C mismatches. It is worthy of note that both the association and dissociation kinetics of 7-AM-ACTD in self-complementary oligomer solutions are considerably slower (some are almost an order of magnitude slower) than the parent ACTD but only moderately so for the mismatched oligomers (compare Tables 2 and 3). This resulted in a much slower 7-AM-ACTD dissociation rate from -TGCA-sequence than from the T/T-mismatched site, despite the comparable dissociation rates for the parent ACTD.

Discussion. In summary, comparative electrophoretic, thermal denaturation, and spectroscopic studies with dodecamers of the form d(AAAA-XGCX-TTTT) and the corresponding self-complementary counterparts suggest that despite the considerable decrease in dimeric duplex stability, ACTD binds strongly to the GC sequence with flanking T/T or C/C mismatches but weakly to the one with G/G or A/A mismatches. The relative binding order is found to be: T/T > C/C >> G/G > A/A. Spectral titrations indicate that the binding affinities of the T/T and C/C-mismatched dodecamers do not differ greatly from each other and are comparable to or even stronger than the corresponding self-complementary -XGCY- sequences. In contrast to the self-complementary dodecamers, the Scatchard plots for the T/T- and C/C-mismatched oligomers exhibit unusual curvatures. Excellent fits of these unusual binding isotherms, however, are obtained with a model assuming that ACTD only binds to the dimeric duplex form which is in dynamic equilibrium with the monomeric hairpin conformation. The dodecamer with T/T mismatches, however, exhibits surprisingly slow ACTD dissociation kinetics with a rate about an order of magnitude slower than the oligomer with C/C mismatches and is comparable to the -TGCA- or -AGCT-containing sequence. These results are corroborated by fluorescence measurements using 7-amino-ACTD, a fluorescent analog of ACTD. Fluorescence and absorbance spectral characteristics further indicate that the binding mode of the GC site with flanking T/T or C/C mismatches resembles those of the strong self-complementary -XGCY-containing sequences which are known to be intercalative in nature.

The slow ACTD dissociation rate exhibited by the dodecamer containing T/T mismatches is rather unexpected, especially since it is comparable to that of the slow dissociating -TGCA-containing dodecamer. One would have anticipated that the dimeric duplex destabilization caused by the presence of mismatched bases would have resulted in a very rapid drug dissociation. The observation of a slow dissociation rate, thus, suggests that the T/T mismatches flanking the duplex 5'GC3' site provide a very favorable minor groove environment for interactions with the pentapeptide rings of ACTD. In this connection, it may also be interesting to note that dodecamers with pur/pur mismatches exhibit poor ACTD binding, likely the consequence of larger purine bases to result in more distorted minor groove environment, with the consequence of unfavorable interactions with the pentapeptide rings.

The unusual curvatures in the Scatchard plots exhibited by the T/T and C/C mismatched dodecamers are also worth commenting on. This behavior may be understood using the model presented earlier in which the monomeric hairpin and dimeric duplex conformations are in dynamic equilibrium and ACTD only binds to the dimeric form. It can be shown that the Scatchard equation is now modified to:

$$r/m = K_a (n - n L / L_t - r),$$

where r , m and n were defined in Fig. 2 legend and L is the monomeric hairpin concentration. Thus, if the dimeric duplex predominates then L/L_t approaches zero and the equation reduces to the regular one with the saturation binding density extrapolating to n . However, if the hairpin predominates then the L/L_t approaches unity and the plot will move towards the origin. Thus, the exhibited unusual curvatures with the appearance of data points emanating from the origin can be seen as the consequence of the fact that the initial titration points correspond to dilute DNA concentrations where monomeric hairpin conformations predominate but eventually revert to "normal" Scatchard plot at higher DNA concentrations.

It was noted earlier that the ACTD association kinetic trace for the dodecamer containing T/T mismatches requires a 2-exponential fit with a significant contribution from a slow component. The presence of this slow contribution may be the consequence of allosteric conversion from hairpin form to dimeric duplex for further ACTD binding. This is supported by an association kinetic measurement with a decamer d(ATA-TGCT-TAT) which is shown to exhibit predominant dimeric duplex conformation (gel results not shown) and single-exponential association kinetics without the presence of a slow component.

As expected, the association as well as dissociation kinetics of 7-AM-ACTD are slower than those of ACTD. This is consistent with the intercalative binding mode and the slight steric hindrance due to the presence of the amino group at the 7-position. Such differences in kinetic behaviors are quite significant for the self-complementary sequences but are not as apparent for dodecamers with T/T and C/C mismatches. This may likely be attributed to much lower duplex stabilities of the dimeric species and their drug complexes so that the hindrance presented by the 7-amino group becomes less critical.

Although the focus of this study is on the GC sequence with flanking homobase mismatches, our results on the self-complementary dodecamers containing -XGCTY-sequences are also of some interest. The dodecamer results are in general agreement with similar studies using decamers of the form d(ATA-XGCTY-TAT) (Chen, 1988b). The relative ACTD binding affinities are found to be: -TGCA- > -CGCG- > -AGCT- >> -GGCC-, whereas the rate of ACTD dissociation is in the order: -TGCA- < -AGCT- < -CGCG- << -GGCC-, with TGCA- exhibiting the slowest dissociation kinetics. The fact that ACTD binds weakly and dissociates very rapidly from a GC site with adjacent G•C base pairs or G/G mismatches suggest that the 2-amino group of guanine which resides at the minor groove may be the culprit for the unfavorable interactions with the pentapeptide rings of the drug. Indeed, the much weaker intensity of the drug-retarded eletrophoretic band for the -CGCG- as opposed to those of -TGCA- and -AGCT- sequences (results not shown) is the consequence of its much faster dissociation rate.

Is the Strong Binding of Actinomycin D to d(CGTCGACG) the Consequence of End-Stacking?

As mentioned in the introduction, it has recently been reported that ACTD binds strongly and cooperatively to a non-GC containing self-complementary octamer d(CGTCGACG) with a 2:1 drug to duplex ratio (Synder et al., 1989). However, if one is

to view the classic intercalative preference of the 5'GpC3' sequence to be that of ACTD intercalating at G3'p5'C, it follows that the drug favors stacking and hydrogen bonding at a G•C base pair on the 3' side of dG. Thus, there exists the possibility that the drug molecules may in fact stack on the G•C base pairs at both ends of this oligomeric duplex rather than binding at the internal non-GC sequences. To investigate this possibility, d(CGTCGACG) and several related oligomers resulting from replacing or appending the terminal base(s) of this octamer with dT and/or dA are used in a comparative study employing equilibrium titration, thermal denaturation, circular dichroic, and stopped-flow kinetic measurements.

The oligomers chosen are: d(XGTCGACY) in which X = A, T, G, or C and d(X-CGTCGACG), d(CGTCGACG-Y), and d(X-CGTCGACG-Y) in which X is A or T and Y being complementary to X. It is reasoned that if end-stacking of ACTD on the 3' side of dG is the culprit, the replacement of the terminal dG by another base and a concomitant complementary replacement at the other end will lead to a considerable reduction in the ACTD binding affinity. In contrast, minimal alteration in binding characteristics should result if it is due to the internal sequence binding. Such a rationale should be particularly valid for the base-added oligomers where the entire 8 base-paired duplex is now intact with only a dangling base or a base-pair being appended to each end. On the other hand, significant effects on the binding behaviors will be expected for these oligomers if end-stacking mechanism is operative. Additional studies were also made with d(CGACGTCG) by simply switching the A, T pair of the parent octamer without altering the terminal bases and should thus retain its end-stacking abilities.

Equilibrium Binding Titrations.

Qualitative Binding Order. As described earlier, a comparison of absorbance difference spectra at a given P/D ratio, where P and D are nucleotide and drug concentrations, respectively, can provide qualitative ACTD binding order for these oligomers. Representative absorbance difference spectra at P/D = 10 are compared in Figure 7 for these oligomers. It is apparent that the qualitative ACTD binding order for the d(XGTCGACY) series (panel A) is: d(CGTCGACG) > d(GGTCGACC) > d(TGTCGACA) ≥ d(AGTCGACT). On the other hand, the order for the oligomers containing terminally-added base(s) of dA and/or dT (panel B) is found to be: d(CGTCGACG) > d(CGTCGACG-T) ≥ d(A-CGTCGACG) > d(CGTCGACG-A) ≥ d(T-CGTCGACG) ≅ d(A-CGTCGACG-T) > d(T-CGTCGACG-A). It is apparent that the replacement and blocking of the 5'-end of dC and/or 3'-end of dG had considerably diminished the oligomer's ability to bind ACTD. In addition, the binding affinities are strongly dependent on the nature and the location of the replacing / blocking base(s). The moderate ACTD binding to d(GGTCGACC) most likely is the consequence of binding to the GG/CC sequence.

Scatchard Plots. To obtain more quantitative binding parameters, results of spectral titrations were converted to binding isotherms. Scatchard plots were constructed using absorbance differences between 427 and 480 nm and representative plots are shown in Figure 8. It is apparent that the plot for d(CGTCGACG) is decidedly curved and its binding parameters cannot be obtained via linear least-squares fits. It is also clear that the replacement of the terminal bases had significantly diminished binding affinities, as

evidenced by the much reduced slopes (panel A). Their binding constants were estimated from linear least-squares fits and their values are included in Table 4. Effects due to the terminal addition with A and/or T base(s) can be seen in panel (B) where representative plots are compared with the parent octamer. Although the weaker binding plots appear to be linear, the stronger binding ones are decidedly curved. Thus, a more straightforward approach was taken by directly fitting the experimental binding isotherms with a binding model.

Fitting the Binding Isotherms with a Binding Model. If ACTD were to bind via end-stacking, two binding sites are available. Thus, the following binding model was assumed:



where S and L_2 represent the drug and oligomeric duplex, respectively. With use of mass balances of the DNA and drug concentrations, the following equations can be derived:

$$K_1 K_2 S^3 + [K_1 K_2 (L_t - S_t) + K_1] S^2 + [K_1 (0.5 L_t - S_t) + 1] S - S_t = 0 \quad (1)$$

$$L_2 = (L_t - S_t + S) / (2 + K_1 S) \quad (2)$$

$$\Delta A = \epsilon_S [+ \epsilon_1 K_1 L_2 (1 + 2 K_2 S)] S \quad (3)$$

where ΔA is the observed absorbance difference between 427 and 480 nm. ϵ_S , and ϵ_1 are extinction coefficients of the free and bound drugs, respectively. L_t and S_t are the respective total DNA oligomeric (in strand) and drug concentrations. These equations were used to extract binding parameters via nonlinear least-squares fits on the experimentally observed data. As can be seen in Figure 9, excellent fits are obtained for most of the binding isotherms and the extracted binding parameters from these fits are included in Table 4 for comparison. Of particular interest are the values found for d(CGTCGACG) of 1×10^5 and $3.2 \times 10^7 \text{ M}^{-1}$ for the binding constants K_1 and K_2 , respectively. The highly cooperative nature of ACTD binding to this octamer is confirmed by $K_2 \gg K_1$ in which binding of the second drug is much stronger than that of the first. Although a good nonlinear least-squares fit does not guarantee the correctness of the model, the finding of a highly cooperative binding for the parent octamer and the considerably reduced binding affinities and cooperativities for the terminally replaced or base-added oligomers suggest the plausibility of the assumed model. It is interesting to note that significant binding affinity and cooperativity are retained in d(CGTCGACG-T) and d(CGTCGACG-A) (see Table 4).

Thermal Denaturation Measurements.

The extent of melting temperature increases upon drug binding can also provide information on the drug binding affinity of a DNA. Melting temperatures of the oligomers and the increases upon ACTD binding are also included in Table 4 for comparison. It is apparent that the pattern of melting temperature increases is in general agreement with that of binding affinities. For example, the ACTD-induced melting temperature increase is about 20 °C for d(CGTCGACG), whereas it is less than 10 °C for

any of the terminally replaced oligomer, in agreement with their much reduced binding affinities. In addition, the base-added oligomers exhibit somewhat smaller melting temperature increases than that of the parent octamer. Consistent with the retention of significant binding affinity and cooperativity, a dT or dA addition to the 3' end of dG resulted in the largest drug-induced duplex stability among the derived oligomers.

Stopped-Flow Kinetic Measurements via Absorbance Monitoring.

Association Kinetics. Association kinetic measurements were made by mixing equal volumes of 8 μ M ACTD and 100 μ M (nucleotide) DNA in a stopped-flow rapid-scanning instrument. Representative kinetic profiles with 428-nm absorbance monitoring are shown in Figure 10 and the results of 1- or 2-exponential fit along with their total absorbance changes are compared in Table 5. As can be seen from Figure 10A, the two oligomers with terminal A•T base pair replacement exhibit small absorbance changes and fast association kinetics with characteristic times of around 0.25 s at 20 °C. Despite an observed significant total absorbance change, the oligomer d(GGTCGACC) exhibits an even faster association kinetics, with a measured slowest association characteristic time of around 0.04 s. In contrast, nearly 50% of the absorbance changes were measurable by the stopped-flow technique for d(CGTCGACG), with the bulk of the measured changes exhibiting the slow characteristic association time of around 14 s. Interestingly, oligomers with bases added to both ends exhibit significantly smaller total absorbance changes and slower association kinetics than those of oligomers with a dangling base which in turn are slower than the parent octamer. It should also be noted that the two oligomers with respective dangling dT and dA added to the 3' end of dG exhibit the largest absorbance changes for the slow association component (see panels B and C). It is also worth noting that the magnitudes of the total absorbance change ΔA_t (see Table 5) are in general agreement with the qualitative binding orders established in the earlier section.

Dissociation Kinetics. SDS-induced ACTD dissociation kinetics were also measured at 20 °C. The results indicate that in the d(XGTCGACY) series, only the parent octamer d(CGTCGACG) exhibits a slow enough dissociation kinetics to be measured by the stopped-flow technique to yield a characteristic dissociation time of 0.8 s. Except for d(CGTCGACG-T), the considerably smaller binding-induced total absorbance changes of the base-added oligomers prevented us from obtaining meaningful dissociation kinetic profiles. Nevertheless, a dissociation time of about 1.3 s is obtained for the base-added oligomer d(CGTCGACG-T) which is slower than that of the parent octamer.

Circular Dichroic Spectral Characteristics.

Binding of ACTD to DNA induces a characteristic positive and negative CD maxima near 293 and 270 nm, respectively. Thus, the extent of induced CD intensity at these wavelengths can be used to provide qualitative binding information. Representative CD difference spectra (drug/DNA - DNA) are compared in Figure 11. Consistent with the absorbance results, d(CGTCGACG) exhibits the largest CD intensity enhancement at 293 nm. Much weaker CD intensities were induced at this wavelength for the end-base replaced oligomers (panel A). The distinctly different induced CD spectral characteristics can also clearly be seen. The progressive reduction of the 293-nm CD intensity on the base-added oligomers are also apparent (panels B and C). Thus, the CD measurements

are in general agreement with the binding order established earlier via absorbance titrations. CD spectral measurements in the 520 - 320 nm region were also made to indicate weak broad positive maxima near 460 nm (not shown), in agreement with that of Snyder et al. (1989).

Fluorescence Spectral Enhancement of 7-Amino-ACTD.

Emission Spectral Characteristics. Binding of 7-AM-ACTD to an oligomeric duplex containing a GpC sequence usually results in a strongly enhanced fluorescence emission spectrum exhibiting a maximum at 650 nm and a shoulder near 610 nm. Fluorescence intensity enhancement patterns for 7-AM-ACTD upon binding to d(CGTCGACG) and the related oligomers are compared in Figure 12 as difference spectra (ACTD/DNA - ACTD). It is immediately apparent that in contrast to the GpC containing oligomers, d(CGTCGACG) and the base-added oligomers induced a much stronger fluorescence enhancement at 610 nm than at 650 nm to result in a double-humped spectral pattern with the intensity of the former now becomes larger than that of the latter. Panel (A) compares the effect of adding dA to the 5' terminal and/or dT to the 3' terminal of the parent octamer on the fluorescence spectral patterns of 7-AM-ACTD. Consistent with its weaker ACTD binding, d(A-CGTCGACG) induces a smaller fluorescence intensity enhancement than that of d(CGTCGACG). In contrast, a dramatic intensity enhancement much more than the parent octamer is induced by d(CGTCGACG-T) and despite its considerably weaker binding affinity, d(A-CGTCGACG-T) induces nearly identical intensity enhancement as that of the parent octamer (panel A). Similarly, d(CGTCGACG-A) induces a stronger fluorescence intensity enhancement than its parent octamer but the effect is not as dramatic as that of dT attachment (see panel B). And again, despite their weaker binding affinities, d(T-CGTCGACG) and d(T-CGTCGACG-A) induced nearly identical fluorescence enhancements as that of the parent octamer. As for the end-base replaced octamers, significantly weaker fluorescence enhancements than the parent octamer were observed (see also panel B).

Fluorescence Kinetic Measurements. In contrast to the small absorbance changes for some of the base-added oligomers, those of the corresponding fluorescence changes are quite considerable even for the oligomers with bases added to both ends. Thus, the slow component of the association kinetics which was barely discernable via absorbance monitoring can now clearly be seen in the fluorescence monitoring. The association kinetic profiles at 20 °C for the base-added oligomers are shown in Figure 13. It is immediately apparent that the association kinetics for the base-added oligomers are considerably slower than those of the parent octamer. In particular, the decamers with terminal A•T base pairs exhibit more than an order of magnitude slower kinetics than the parent octamer. The nonlinear least-squares fitted kinetic parameters with 1- or 2-exponential equation are summarized in Table 6.

SDS-induced dissociation kinetics were also measured. These non-stopped-flow measurable dissociation kinetic profiles can be adequately fitted with single exponential decays and the extracted parameters were also included in Table 6 for comparison. It is apparent that the rates of dissociation for the base-added oligomers are considerably slower than the parent octamer, with strong dependence on the nature and the location of the attached base(s).

Studies with d(CGACGTCTG).

To further support our thesis on end-stacking, studies were also made with d(CGACGTCTG) by merely interchanging the A, T pair of the parent octamer without altering the terminal bases. This oligomer is expected to bind well to ACTD if end-stacking is the culprit. Indeed, it is found that (1) ACTD binds strongly to this oligomer with high cooperativity, as indicated by the considerable curvature of its Scatchard plot (not shown) and the respective values of 1×10^5 and $3.6 \times 10^7 \text{ M}^{-1}$ for K_1 and K_2 (see Table 4) obtained via nonlinear least-squares fit on its binding isotherm using the described binding model; (2) that the ACTD-induced CD exhibits a sizable positive intensity near 293 nm as well as 460 nm; (3) that the melting temperature increase upon drug binding is around 21°C ; and (4) that the characteristic association and SDS-induced dissociation times were estimated to be 0.22 and 0.6 s, respectively. Furthermore, this oligomer induces strong fluorescence intensity enhancement exhibiting a 600-nm maximum (not shown). All these characteristics are very similar to those of the parent octamer d(CGTCGACG).

Discussion

Consistent with previous calorimetric studies of Synder et al. (1989), our equilibrium binding titrations indicate that d(CGTCGACG) binds strongly to ACTD and exhibits very high cooperativity to result in a 2:1 drug to DNA complex. Nonlinear least-squares fits of the experimental binding isotherms with a binding model yielded binding constants of 1×10^5 and $3.2 \times 10^7 \text{ M}^{-1}$ for the 1- and 2-drug binding processes, respectively. In support of our postulate that the strong ACTD binding of this octamer is the consequence of ACTD stacking on the 3'-side of dG at the terminal G•C base pairs, the replacement of G at the 3'-terminal by A, T, or C and the complementary base at the other end resulted in more than an order of magnitude reduction in the binding affinities, the loss of binding cooperativity, the considerably smaller ACTD-induced melting temperature increases, and the much faster drug-DNA association as well as dissociation kinetics. Although the weak binding of d(AGTCGACT), d(TGTCGACA) and even d(GGTCTGACC) which contains as many G•C base pairs as in the parent octamer may partly be due to the decreased duplex stability, as indicated by their lower melting temperatures (see Table 4), the main reason most likely is the absence of dG at the 3'-terminal in these oligomers for the ACTD end-stacking.

To further support our thesis on end-stacking, studies were also made with oligomers by appending dA or dT to the 5' and/or 3' ends. The rationale being that by adding a dT or dA to the terminal(s) without altering the 8-base self-complementary internal sequence, minimal effect on the binding affinity will be expected if binding occurs at the internal sequences. On the other hand, significant alteration on the binding characteristics should occur if end-stacking to the G•C base pairs is the culprit. The results indicate that, in contrast to their parent octamer, these oligomers exhibit significantly weaker ACTD binding affinities with considerably reduced cooperativity as more bases are added. In addition, association kinetic measurements indicate that each end-base-added oligomer exhibits a slow association component which is significantly slower than that of the parent octamer. In particular, the oligomeric duplexes with A•T base pairs at both ends exhibit considerably weaker binding and slower association kinetics than the

corresponding duplexes with a dangling A or T at the end. These results are consistent with the drug molecules stacking at the duplex ends. Interestingly, both the binding and kinetic characteristics are strongly dependent on the nature and the location of the added bases. For example, the (A)-CGTCGACG-(T) series of oligomers exhibit somewhat higher binding affinities than the corresponding (T)-CGTCGACG-(A) counterparts. Significant ACTD binding affinity and cooperativity are retained when dA or dT is added to the 3'-end of dG, whereas weaker binding and cooperativity are apparent for oligomers with dA or dT attached to the 5' end of dC.

Despite the fact that the extent of fluorescence enhancements of 7-amino-ACTD do not exactly correlate well with the binding order of oligomers studied, the fluorescence results appear to provide the most convincing evidence that the binding of ACTD to d(CGTCGACG) occurs at the duplex terminals rather than at the internal sequences. If the binding were to occur at the internal sequences, a dangling base at either end of a duplex is not expected to have a significant influence on the fluorescence spectral characteristics of the bound drug. Yet our results clearly indicate that when the dangling dA or dT is attached to the dG of the 3' terminal, dramatic fluorescence enhancement is observed. In contrast, weak or moderate enhancement is seen when the dangling base is attached to dC at the 5' terminal. The large fluorescence intensity enhancements for the base-appended oligomers provided us with the opportunity to study the SDS-induced dissociation kinetic behaviors of the drug which were not possible with the absorbance monitoring. In addition to confirming the expected slower dissociation rates for the base-added oligomers than their parent octamer, these kinetic results provided us with a powerful argument for the end-stacking mechanism. For example, characteristic times for the dissociation of 7-AM-ACTD from d(CGTCGACG), d(CGTCGACG-T), and d(CGTCGACG-A) are about 1, 3.3, and 26 s, respectively. One would be hard pressed to explain how a dangling A base can induce a 30-fold decrease in the drug's off rate if the binding were at the internal sequences rather than at the ends, and how can a change in the dangling base from A to T result in a rate change of nearly 10-fold. These results can, however, be more easily explained in terms of the drug interacting at the terminal G•C base pairs. The strong fluorescence enhancement is likely the consequence of the drug's experiencing a more hydrophobic environment via wrapping around of the dG-attached dangling A or T base to stack on the benzenoid portion of the phenoxazone ring of ACTD. Such an interpretation is consistent with the observation and interpretation on the splitting of the H7 and H8 NMR proton signals during the ACTD titrations with dinucleotide pdG-dT or pdG-dA (Krugh & Neely, 1973). It is further supported by the earlier fluorescence studies of 7-AM-ACTD (Modest & Sengupta, 1974; Chiao, et al., 1979) indicating that binding of dAMP enhances the fluorescence intensity near 600 nm. The extent of such interactions should be dependent on the nature of the base, with A expected to provide stronger stacking interaction than T.

Another piece of evidence implicating stacking at the dG base comes from the positive sign of the CD band at 460 nm. Binding of ACTD to DNA usually results in a negative intensity in this region except for the binding to mononucleotide pdG (Homer, 1969; Brown & Shafer, 1987). The unusual feature of the positive CD intensity at this wavelength observed for ACTD binding to d(CGTCGACG) was pointed out earlier by

Snyder et al. (1989). It is also interesting to note that the long wavelength CD band of 7-AM-ACTD reverts from negative with intercalative binding of dinucleotide pdG-dC to positive with stacking interactions of pdC-dG (Chiao et al., 1979). Thus, the observation of a positive 460-nm CD band is consistent with ACTD stacking to dG at the duplex ends.

Additional corroborating evidence supporting the notion of ACTD stacking on the 3'-side of dG at the terminal G•C base pairs comes from the study with octamer d(CGACGTCG) in which an alteration in internal sequence is made from the parent oligomer by simply interchanging the A, T pair without disturbing the C and G at the respective 5' and 3' ends. It was found that this octamer exhibits a strong ACTD binding affinity with high cooperativity, a large ACTD-induced melting temperature increase, a significant fluorescence intensity enhancement of 7-AM-ACTD near 600 nm, a positive CD band around 460 nm for the bound ACTD, and relatively slow association as well as dissociation kinetics. These characteristics are very similar to those of the parent d(CGTCGACG) and are consistent with its ability to accommodate ACTD at the duplex ends.

Our results suggest that the binding constant (K_1) for the initial ACTD stacking at one of the terminal is around $1 \times 10^5 \text{ M}^{-1}$, which is more than an order of magnitude higher than binding to mononucleotide pdG (Krugh & Neely, 1973) but about the same order of magnitude lower than intercalation at the GpC sequence of a duplex DNA. The stronger affinity compared to the mononucleotide is most certainly due to the ability of the oligomer to interact with one of the drug's two pentapeptide rings. The weaker binding compared to the intercalation at the duplex GpC site is likely the consequence of the facts that (1) end-stacking only results in the formation of half the number of hydrogen bonds as that of intercalation at the duplex GpC site, (2) only one of the two pentapeptide rings can be anchored at the minor groove, and (3) the fraying of the duplex ends may somewhat hamper the initial ACTD binding. It is, however, more difficult to rationalize the highly cooperative effect of a 300-fold increase in the binding affinity for the second drug ($K_2 = 3.2 \times 10^7 \text{ M}^{-1}$). It may be that the binding of the first drug molecule not only stabilizes the duplex for easier second drug stacking but may have also altered the duplex conformation near the other end, via hydrogen bonding and minor groove - pentapeptide ring interactions, so that hydrogen bonding and minor groove interactions for the second drug molecule become much more favorable. The above two-step process of binding may also account for the observed much slower association kinetics exhibited by d(CGTCGACG) and d(CGACGTCG) than the other XGTCGACY octamers studied, as the weak bindings of these other octamers are most likely at the internal sequences. The slower dissociation kinetics exhibited by the parent octamer may be attributed to the hydrogen bonding with the stacked guanines and minor groove interactions with one of the two pentapeptide rings, similar to those observed for intercalative binding at the GpC site. The observation of an association or dissociation process slower than that of the parent octamer for each of the (X)-CGTCGACG-(Y) series of oligomers is consistent with the varying degrees of interference by the dangling bases or A•T base pairs.

Finally, it should be noted that Snyder et al. (1989) have also studied d(CGTACG) and d(CATCGATG) and found the binding constants to be 3.3×10^5 and $7.1 \times 10^5 \text{ M}^{-1}$,

respectively. Weaker bindings were also found for d(CTAGATCTAG) and d(CGTTAACG) with corresponding binding constants of $<7.4 \times 10^4$ and $<3.1 \times 10^4 \text{ M}^{-1}$, respectively. Since end-stackings can occur with these oligomers, their weaker ACTD binding require further elaboration. The weaker ACTD affinities of d(CGTACG), d(CATCGATG), and d(CGTTAACG) may partly be attributed to lower duplex stabilities due to shorter oligomer and/or less number of G•C base pairs as compared to the parent octamer so as to disfavor the stacking and hydrogen-bonding interactions at the terminals. As to the weaker binding of d(CTAGATCTAG), it may be the consequence of its longer sequence without additional G•C base pairs to result in a significant contribution from the hairpin conformation. The hairpin will only have a single end-stacking site with no possibility of exhibiting cooperative binding.

Binding of Actinomycin D to Hairpins with GC-Containing Stems.

Characteristics of actinomycin D (ACTD) binding to DNA hairpins containing a GC sequence at the stem were studied with use of exclusively hairpin-forming decamers of the form d(GCX-TTTT-YGC) and d(XGC-TTTT-GCY), where X and Y are complementary to each other. Spectral titrations, circular dichroic measurements, and melting experiments revealed that all the hairpins studied exhibit strong ACTD binding affinity. All Scatchard plots appear to be roughly linear and converge to a saturation binding density of about 1 drug molecule per strand. The binding constants extracted from linear least-squares fits range from 1.1×10^7 to $3.3 \times 10^7 \text{ M}^{-1}$, except for d(GCC-TTTT-CGG) which exhibits the weakest affinity of $4 \times 10^6 \text{ M}^{-1}$. Stopped-flow kinetic measurements indicate that although the kinetics of association do not exhibit definite patterns or trends for the two series, those of SDS-induced dissociation are significantly different. The XGC-TTTT-GCY oligomers exhibit considerably slower dissociation rates than those of GCX-TTTT-YGC series. Such kinetic differential may be the consequence of the ability of the hairpin loop to provide significant interactions with one of the pentapeptide rings of the drug in the d(XGC-TTTT-GCY) series, in addition to the other pentapeptide ring interacting at the minor groove of the X•Y base-pair, whereas ACTD binding to the duplex stem of d(GCX-TTTT-YGC) results in one of the two pentapeptide rings of the drug dangling with no anchorage.

Binding of Actinomycin D to Hairpins with Non-GC-Containing Stem.

Binding of ACTD to hairpins with non-GC-containing stem was studied with oligomers of the form d(GXY-TTTT-Y'X'C), where X' and Y' are complementary to X and Y, respectively. The choice of a G•C base pair at the terminal is to enhance the hairpin formation and to reduce the end-fraying effect. Although the absorbance intensity changes due to ACTD binding are not as large as those of the GC containing hairpins, significant spectral changes were observed for most of the non-GC containing hairpins. Comparison of absorbance difference spectra (ACTD/DNA - ACTD) suggests the following qualitative ACTD binding order for the hairpin stem sequences to be: GGG > GAC > GGA, GGT \geq GTC \geq GTG > GAG >> GAT, GTA, GTT > GAA. The stem containing 3 G•C base pairs exhibits the largest spectral changes which is followed by sequences with 2 G•C base pairs and then stems with a single G•C base pair, with GAA exhibiting negligible alteration. Binding parameters extracted via linear least-squares

fits of Scatchard plots suggest that except for d(GGG-TTTT-CCC) which exhibits a binding constant of $6.1 \mu\text{M}^{-1}$, the ACTD binding affinities of these oligomers are lower than that of the weakest GC-containing hairpin d(GCC-TTTT-GGC). The oligomers containing two G•C base pairs in the stem exhibit binding strengths ranging from 0.6 to $4 \mu\text{M}^{-1}$. Much weaker binding affinities are observed for oligomers containing a single G•C base pair in the duplex stem. Except for d(GGG-TTTT-CCC), all oligomers studied exhibit characteristic association times of $< 0.085 \text{ s}$ by mixing equal volumes of $100 \mu\text{M}$ nucleotide and $8 \mu\text{M}$ ACTD solutions. The hairpin with a GGG stem exhibits nearly an order of magnitude slower association life time of around 0.61 s . Except for three hairpins, all oligomers studied exhibit detergent-induced dissociation rate constants greater than 25 s^{-1} . Hairpins containing GGG, GTC, and GAC stems exhibit dissociation rate constants of 0.46, 0.83, and 1.2 s^{-1} , respectively. Consistent with significant ACTD binding affinities of hairpins with two or more G•C base pairs in the stem, these oligomers exhibit melting temperature increases of 15 or more degrees, whereas those with stems containing a single G•C base pair exhibit negligible melting temperature increases upon drug binding.

These results on the ACTD binding to hairpins are currently being organized and analyzed to provide for a consistent interpretation.

Acid-facilitated Supramolecular Assembly of G-quadruplexes in d(CG₃G)₄

Guanine is unique among the four DNA bases by virtue of its four hydrogen bonding sites being strategically distributed in such a way that four G bases can readily form 8 hydrogen bonds to result in a cyclic base-quartet. Thus, a DNA sequence with a stretch of G's can form a four-stranded helical structure called G-quadruplex which is of current intense interest. This interest has been further stimulated by the possible relevance of such structures in the recombinational events at the immunoglobulin switching regions as well as in telomeric functions. Effects of monovalent cations on the G-quadruplex structural formation of telomeric DNA sequences have been extensively studied in recent years. Evidence suggests that due to its optimal size, K^+ is much more effective in stabilizing G-quadruplex formation. The ion is found to be sandwiched between two G-tetrads to form an octa-coordination complex with the carbonyl groups of guanines. It was also found that for a contiguous guanine oligomer, the parallel strand orientation is thermodynamically more favorable than the anti-parallel conformation.

We have recently found that molar $[\text{K}^+]$ induces aggregate formation in d(CG₃G)₄, as evidenced by absorbance, circular dichroic, and gel measurements. The kinetics of this transformation are extremely slow at pH 8 but are found to be greatly facilitated in acidic conditions. Kinetic profiles via absorbance or CD monitoring at single wavelength resemble those of autocatalytic reacting systems with characteristic induction periods. More than 1 M KCl is needed to observe the onset of aggregation at 20°C and pH 5.4 within the time span of one day. Time dependent CD spectral characteristics indicate the formation of parallel G-tetraplexes prior to the onset of aggregation. Despite the evidence of K^+ -induced parallel G-quadruplex and higher molecular weight complex formation, both d(TGG)₄ and d(CG₃G)₄T fail to exhibit the observed phenomenon, thus, strongly implicating the crucial roles played by the terminal G and base protonation of

cytosines. A plausible mechanism for the formation of a novel self-assembled structure is speculated: Aided by the C⁺•C base pair formation, parallel quadruplexes are initially formed and subsequently converted to quadruplexes with contiguous G-tetrads and looped-out cytosines due to high [K⁺]. These quadruplexes then vertically stack as well as horizontally expand via inter-quadruplex C⁺•C base pairing to result in dendrimer-type of self-assembled super structures. The presence of ACTD inhibits the K⁺-induced aggregate formation, suggesting strong binding of CGG trinucleotide repeats to ACTD at low salt conditions. The article which describes these results has just appeared in print: Chen, F.-M. (1995) *J. Biol. Chem.* 270, 23090-23096.

CONCLUSION

We believe the works completed thus far on ACTD are essential and have laid a good foundation for our future study on the synergistic effects of drugs. Our next step will be to carry out similar sequence specificity studies on the other two drugs, chromomycin A₃ and distamycin A. The results of these individual drug studies will then form the bases for designing the study on synergism.

REFERENCES

- Aivasashvilli, V. A., & Beabealashvilli, R. S. (1983) *FEBS Lett.* 160,124-128.
- Akiyama, M., Maki, H., Sekiguchi, M., & Horiuchi, T. (1989) *Proc. Natl. Acad. Sci. U.S.A.* 86,3949-3952.
- Bailey, C., Graves, D. E., Ridge, G., & Waring, M. J. (1994) *Biochemistry* 33, 8736-8745.
- Bailey, S. A., Graves, D. E., & Rill, R. (1994) *Biochemistry* 33, 11493-11500.
- Bailey, S. A., Graves, D. E., Rill, R., & Marsch, G. (1993) *Biochemistry* 32,5881-5887.
- Brown, S. C., Mullis, K., Levenson, C., & Shafer, R. H. (1984) *Biochemistry* 23, 403-408.
- Brown, D. R., Kurz, M., Kearns, D. R., & Hsu, V. L. (1994) *Biochemistry* 33,6516-64.
- Chen, F.-M. (1988a) *Biochemistry* 27,1843-1848
- Chen, F.-M. (1988b) *Biochemistry* 27, 6393-6397.
- Chen, F.-M. (1992) *Biochemistry* 31, 6223-6228.
- Chiao, Y.-C. C., Rao, G., Hook III, J. W., & Krugh, T. R. (1979) *Biopolymers* 18, 1749-1762.
- Chu, W., Shinomiya, M., Kamitori, K., Kamitori, S., Carlson, R. G., Weaver, R. F., & Takusagawa, F. (1994) *J. Am. Chem. Soc.* 116, 7971-7982.
- Fassman, G. D. (ed) (1975) *CRC Handbook of Biochemistry and Molecular Biology*, 3rd Ed., Vol. I, p.589, CRC Press, Cleveland, OH.
- Fletcher, M. C. & Fox, K. R. (1993) *Nucleic Acids Res.* 21, 1339-1344.
- Fox, K. R., & Waring, M. J. (1984) *Nucleic Acids Res.* 12, 9271-9285.
- Goodisman, J., Rehfuess, R., Ward, B., and Dabrowiak, J. C. (1992) *Biochemistry* 31,1046-1058.
- Goodisman, J., & Dabrowiak, J. C. (1992) *Biochemistry* 31, 1058-1064.

- Homer, R. B. (1969) *Arch. Biochem. Biophys* 129, 405-407.
- Hunter, W. (1992) *Methods in Enzymology* 211, 221-231.
- Kamitori, S., & Takusagawa, F. (1994) *J. Am. Chem. Soc.* 116, 4154-4165.
- Kamitori, S., & Takusagawa, F. (1992) *J. Mol. Biol.* 225, 445-456.
- Krugh, T. R. (1972) *Proc. Nat. Acad. Sci. USA* 69, 1911-1914.
- Krugh, T. R., & Neely, J. W. (1973) *Biochemistry* 12, 4418-4425. Krugh, T. R., & Neely, J. W. (1973) *Biochemistry* 12, 4418-4425.
- Krugh, T. R., Mooberry, E. S., & Chiao, Y. -C. C. (1977) *Biochemistry* 16, 740-755.
- Lane, M. J., Dabrowiak, J. C., Vouurrnakis, J. N. (1983) *Proc. Natl. Acad. Sci. U.S.A.* 80,3260-3264.
- Liu, X., Chen, H., & Patel, D. J. (1991) *J. Biomol. > NMR* 1, 323-347.
- Modrich, P. (1987) *Annu. Rev. Biochem.* 56,435-466.
- Modest, E. J., & Sengupta, S. K. (1974) *Cancer Chemother. Rep.* 58, 35-48.
- Muller, W., & Crothers, D. M. (1968) *J. Mol. Biol.* 35, 251-290.
- Patel, D. J. (1974) *Biochemistry* 13, 2396-2402.
- Rill, R. L., Marsch, G. A., & Graves, D. E. (1989) *J. Biomol. Struct. Dyns.* 7, 591-604.
- Reh fuss, R., Goodisman, J., & Dabrowiak, J. C. (1990) *Biochemistry* 29, 777-781.
- Scamrov, A. V., & Beabealashvilli, R. Sh. (1983) *FEBS Lett.* 164, 97-101.
- Scott, E. V., Jones, R. L., Banville, D. L., Zon, G., Marzilli, L. G., & Wilson, W. D. (1988) *Biochemistry* 27, 915-923.
- Snyder, J. G., Hartman, N. G., D'Estantoit, B. L., Kennard, O., Remeta, D. P., & Breslauer, K. J. (1989) *Proc. Natl. Acad. Sci. USA* 86, 3968-3972.
- Sobell, H. M., & Jain, S. C. (1972) *J. Mol. Biol.* 68, 21-34.
- Sutherland, G. R. & Richards, R. I. (1994) *Am. Scientist* 82, 157.
- Takusagawa, F., Dabrow, M., Neidle, S., & Berman, H. M. (1982) *Nature* 296, 466-469.
- Van Dyke, M. W., & Dervan, P. B. (1983) *Nucleic Acids Res.* 11, 5555-5567.
- Van Dyke, M. W., Hertzberg, R. P., & Dervan, P. B. (1983) *Proc. Natl. Acad. Sci. U.S.A.* 79,5470-5474.
- Wadkins, R. M., & Jovin, T. M. (1991) *Biochemistry* 30, 9469-9478.
- Waring, M. (1970) *J. Mol. Biol.* 54, 247-279.
- Waterloh, K., & Fox, K. R. (1992) *Biochim. Biophys. Acta* 1131, 300-306.
- White, R. J., & Phillips, D. R. (1989) *Biochemistry* 28,6259-6269.
- Zhou, N., James, T. L., Shafer, R. H. (1989) *Biochemistry* 28, 5231-5239.

Table 1. Comparison of Melting and ACTD Binding Parameters for Dodecamers.

Oligomer	K (μM^{-1})	n / duplex	t_m^0 ($^{\circ}\text{C}$) ^a	t_m ($^{\circ}\text{C}$) ^b
d(AAAA-TGCA-TTTT)	7.5	1.2	35.0	45.7
d(AAAA-AGCT-TTTT)	1.8	1.2	34.8	43.4
d(AAAA-CGCG-TTTT)	3.2	1.2	41.9	56.2
d(AAAA-GGCC-TTTT)	<0.1	-	44.0	45.0
<hr/>				
d(AAAA-AGCA-TTTT)	<0.1	-	<10	-
d(AAAA-TGCT-TTTT)	5.1	0.84	<10	32.8
d(AAAA-GGCG-TTTT)	<0.4	-	~11	20.1
d(AAAA-CGCC-TTTT)	4.3	0.78	<10	28.3

^a t_m^0 is the estimated dimeric duplex melting temperature of 40 μM DNA (nucleotide) via 275-nm monitoring in pH 8 buffer containing 0.1 M NaCl.

^b t_m is the melting temperature of 40 μM DNA (nucleotide) in the presence of 5 μM ACTD.

Table 2. Comparison of Non-Stopped-Flow Measurable ACTD Association and Dissociation Kinetics for Selected Dodecamers at 20 °C.

Oligomer	k_a (min ⁻¹)	k_d (min ⁻¹)
d(AAAA-TGCA-TTTT)	1.44	0.035
d(AAAA-AGCT-TTTT)	0.64	0.047
d(AAAA-CGCG-TTTT)	1.35	0.17
d(AAAA-GGCC-TTTT)	-	5
-----	-----	-----
d(AAAA-AGCA-TTTT)	-	0.7
d(AAAA-TGCT-TTTT)	0.62	0.052
d(AAAA-GGCG-TTTT)	-	-
d(AAAA-CGCC-TTTT)	1.76	0.45

Table 3. Comparison of 7-AM-ACTD Association and Dissociation Kinetics of Dodecamers at 20 °C.

Oligomer	k_a (min ⁻¹)	k_d (min ⁻¹)
d(AAAA-TGCA-TTTT)	0.12	0.0044
d(AAAA-AGCT-TTTT)	0.07	0.011
d(AAAA-CGCG-TTTT)	0.22	0.033
d(AAAA-GGCC-TTTT)	4.6	1.3
-----	-----	-----
d(AAAA-AGCA-TTTT)	-	-
d(AAAA-TGCT-TTTT)	0.33	0.048
d(AAAA-GGCG-TTTT)	6	6
d(AAAA-CGCC-TTTT)	1.2	0.39

Table 4. Summary of Binding and Melting Parameters.

DNA Oligomer	K_a (μM^{-1})	K_1 (μM^{-1})	K_2 (μM^{-1})	T_m^0 ($^{\circ}\text{C}$)	ΔT_m ($^{\circ}\text{C}$)
CGACGTCG	-	0.08	35.6	42	21
AGTCGACT	< 0.1	-	-	36	6
TGTCGACA	< 0.1	-	-	34	9
GGTCGACC	0.38	-	-	40	6
CGTCGACG	-	0.11	31.5	45	20
A-CGTCGACG	-	0.87	0.80	49	14
CGTCGACG-T	-	0.70	4.16	45	18
A-CGTCGACG-T	-	0.56	0.15	52	14
T-CGTCGACG	-	0.22	0.94	47	13
CGTCGACG-A	-	0.03	7.96	45	16
T-CGTCGACG-A	-	0.03	0.96	50	11

K_a is the binding constant estimated via linear least-squares fit of the Scatchard plot. K_1 and K_2 are association constants for binding the first and second drug molecules, respectively. The values are extracted via nonlinear least-squares fit using equations 1-3 in the text.

T_m is the melting temperature of 40 μM (nucleotide) oligomeric solution and ΔT_m is the melting temperature increase in the presence of 7 μM ACTD.

Table 5. Summary of Association Kinetic Parameters.

DNA Oligomer	τ_f (s)	% (fast)	τ_s (s)	% (slow)	ΔA_t
CGACGTCG	0.22 ± 0.03	6.1	10.3 ± 0.2	36.5	0.0386
AGTCGACT	0.26 ± 0.02	62.8			0.0156
TGTCGACA	0.24 ± 0.01	69.4			0.0170
GGTCGACC	0.04 ± 0.003	42.1			0.0335
CGTCGACG	0.14 ± 0.02	4.8	14.1 ± 0.4	42.4	0.0397
A-CGTCGACG	0.17 ± 0.03	8.2	52.6 ± 5.5	7.0	0.0348
CGTCGACG-T	0.15 ± 0.01	6.7	34.5 ± 1.2	50.8	0.0341
A-CGTCGACG-T	0.15 ± 0.03	21.1	222 ± 30	14.9	0.0178
T-CGTCGACG	0.20 ± 0.02	20.3	55.5 ± 3.1	37.7	0.0175
CGTCGACG-A	0.16 ± 0.01	17.3	50.0 ± 2.5	55.9	0.0238
T-CGTCGACG-A	0.15 ± 0.01	34.8	109 ± 2	24.9	0.0140

τ_f and τ_s are the fast and slow components of the 428-nm association kinetic trace as extracted via 1- or 2-exponential fit. ΔA_t is the total absorbance change.

Table 6. Summary of Fluorescence Kinetic Parameters.

DNA Oligomer	τ_1 (s)	% (1)	τ_2 (s)	% (2)	τ_d (s)
CGACGTCG	12.7 ± 0.2	62			~ 1
AGTCGACT	-	-	-	-	-
TGTCGACA	-	-	-	-	-
GGTCGACC	-	-	-	-	-
CGTCGACG	13.7 ± 0.2	57			~ 1
A-CGTCGACG	232 ± 5	~ 100			15.5 ± 1.4
CGTCGACG-T	32.8 ± 0.4	67			3.3 ± 0.1
A-CGTCGACG-T	169 ± 6	18	1640 ± 19	51	7.1 ± 0.5
T-CGTCGACG	150 ± 2	65			19.1 ± 1.2
CGTCGACG-A	59.2 ± 0.4	58			25.6 ± 1.3
T-CGTCGACG-A	119 ± 6	20	813 ± 13	42	16.9 ± 1.2

τ_1 and τ_2 are characteristic association times and τ_d is the characteristic SDS-induced dissociation time.

FIGURE LEGENDS

Figure 1. Comparison of absorption difference spectra (ACTD /DNA - ACTD) at P/D = 40 for self-complementary dodecamers of the form d(AAAA-XGCT-TTTT) (A) and mismatched dodecamers of the form d(AAAA-XGCX-TTTT) (B) at 20 °C.

Figure 2. Comparison of Scatchard plots for three self-complementary and two mismatched dodecamers. Lines correspond to linear least-squares fits on the straight line portions of data points. Absorbance differences between 427 and 480 nm were employed to construct the binding isotherms. Solid lines are those of linear least-squares fit to the simple Scatchard equation $r/m = K_a (n - r)$, where r is the ratio of bound drug to DNA base concentrations, n is the saturation binding density, K_a is the apparent association constant and m is the free drug concentration.

Figure 3. Comparison of equilibrium binding isotherms at 20 °C for d(AAAA-TGCT-TTTT) (squares) and d(AAAA-CGCC-TTTT) (circles) with the fitted curves (solid curves) using the model and equations 1-3 presented in the text. Extracted K_I and K_L are 8.9 and 0.13 μM^{-1} for the T/T whereas 7.4 and 0.07 μM^{-1} for the C/C mismatched oligomers, respectively.

Figure 4. Comparison of CD difference spectra (ACTD /DNA - DNA) of 5 μM ACTD in 40 μM of d(AAAA-TGCT-TTTT) (squares), d(AAAA-CGCC-TTTT) (triangles), d(AAAA-GGCG-TTTT) (diamonds), and d(AAAA-AGCA-TTTT) (circles). Measurements were made with 1-cm cylindrical cells at room temperature.

Figure 5. Representative 1% SDS-induced dissociation kinetic traces at 20 °C with 453-nm absorbance monitoring. d(AAAA-TGCA-TTTT) (squares), d(AAAA-AGCT-TTTT) (diamonds), d(AAAA-CGCG-TTTT) (triangles), d(AAAA-TGCT-TTTT) (solid squares), and d(AAAA-CGCC-TTTT) (solid triangles) solutions. Solid curves are single-exponential fits.

Figure 6. Comparison of fluorescence difference emission spectra at 20 °C of 1.5 μM 7-AM-ACTD in the presence of mismatched and -TGCA- containing dodecamers solutions of 40 μM . Excitation wavelength of 560 nm was used to obtain the spectra.

Figure 7. Absorbance difference spectra (ACTD/DNA - ACTD) for P/D = 10 at 20 °C. (A): Comparison for octamers of the form d(XGTCGACY). (B): Representative plots for oligomers formed by adding dA and/or dT to the terminal(s) of d(CGTCGACG). The difference spectra for oligomers with dA and dT attached to the dC of the 5' terminal are somewhat smaller than the corresponding oligomers with dT and dA attached to the dG of the 3' terminal, respectively, and are thus not shown.

Figure 8. Scatchard plots derived from absorbance titrations at 20 °C. (A): Comparison of the d(XGTCGACY) oligomers. (B): Representative plots for oligomers with dA

and/or dT added to either or both ends of the parent octamer d(CGTCGACG). Absorbance difference between 427 and 480 nm has been used to construct the plots. $[Bound\ drug] / [DNA, nucleotide]$ is designated by r and m represents the free drug concentration.

Figure 9. Comparison of the experimental binding isotherms at 20 °C and the theoretically fitted curves (connected lines) using the binding model and equations 1-3 as described in the text. Panel A: Plots for oligomers of the form (A)-CGTCGACG-(T). Panel B: For oligomers of the form (T)-CGTCGACG-(A) and the parent octamer.

Figure 10. Typical Stopped-flow association kinetic profiles with 428-nm absorbance monitoring at 20°C. Panel A: GGTCGACC (o) and TGTCGACA \cong AGCGACT (Δ). Panel B: Comparison of CGTCGACG and oligomers of the form (A)-CGTCGACG-(T). Panel C: Oligomers of the form (T)-CGTCGACG-(A).

Figure 11. Comparison of difference CD spectra at room temperature for 5 μ M ACTD in 40 μ M/base of oligonucleotide solutions with the contributions due to DNA subtracted. Panel A: Octamers of the form XGTCGACY. Panel B: Oligomers of the form (A)-CGTCGACG-(T). Panel C: Oligomers of the form (T)-CGTCGACG-(A).

Figure 12. DNA-induced fluorescence emission spectral characteristics of 2 μ M 7-amino-ACTD at 20 °C. Panel A: Comparison of the parent octamer and oligomers of the form (A)-CGTCGACG-(T). Panel B: Comparison with oligomers of the form (T)-CGTCGACG-(A) and GGTCGACC.

Figure 13. Association kinetic profiles at 20 °C via fluorescence monitoring at 610 nm of 7-AM-ACTD. Excitation wavelength is at 550 nm. Panel A: Comparison of d(TGTCGACA) \cong d(AGTCGACT) vs. d(GGTCGACC). Panel B: Comparison of d(CGTCGACG) and d(CGACGTCG) vs. d(CGTCGACG-X), where X = A or T. Panel C: Comparison of d(X-CGTCGACG) and d(X-CGTCGACG-Y), where X = A or T and Y is complementary to X.

Figure 1

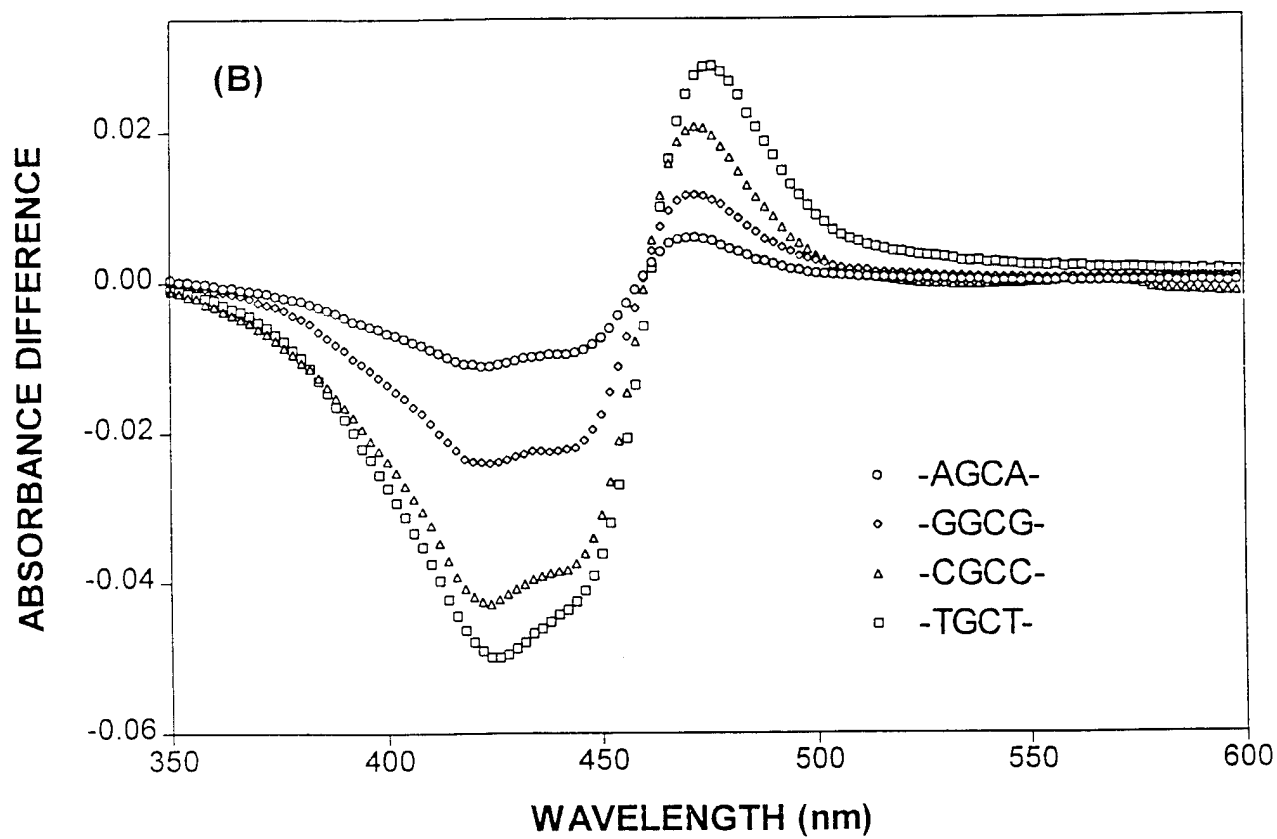
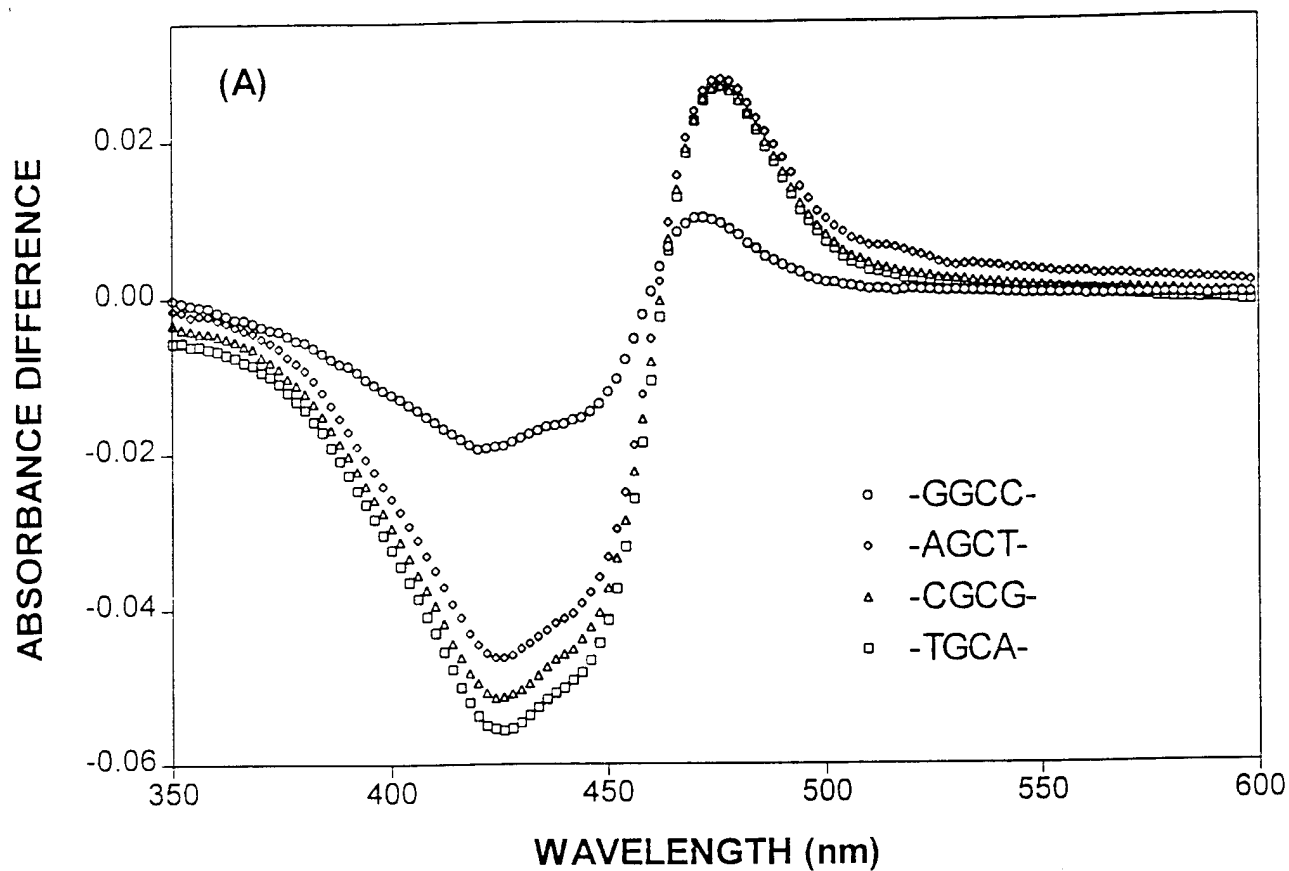


Figure 2

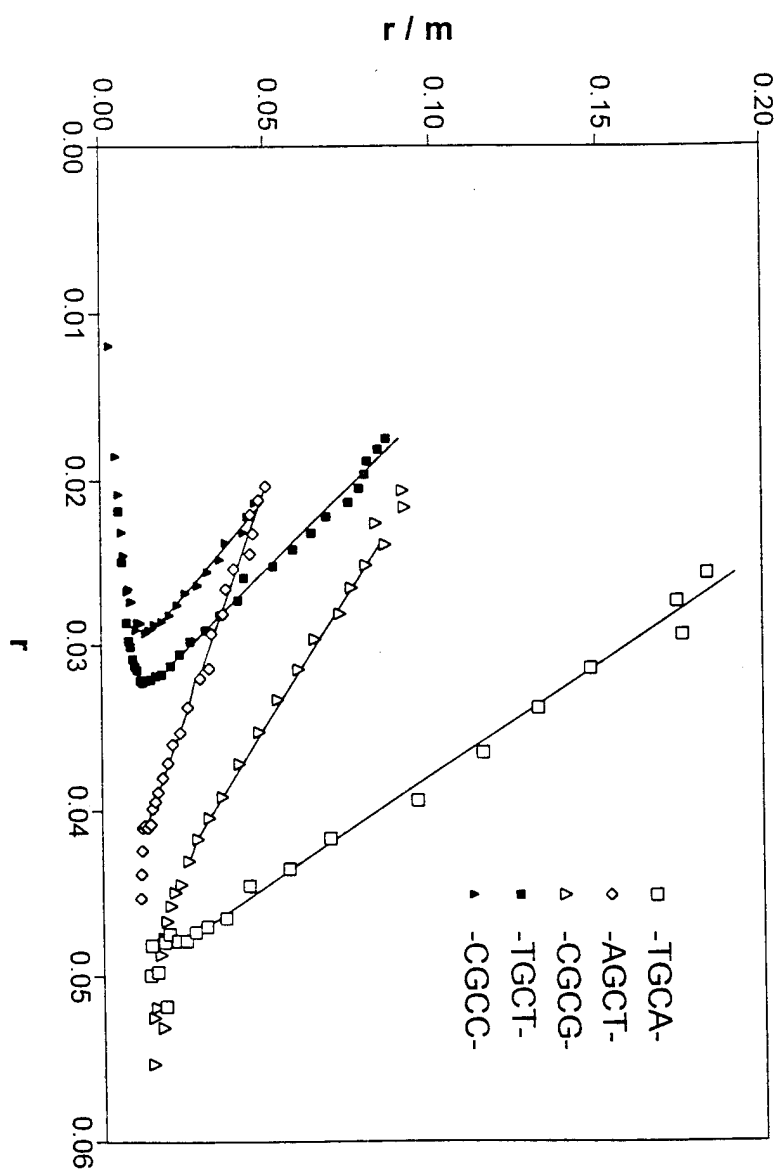


Figure 3

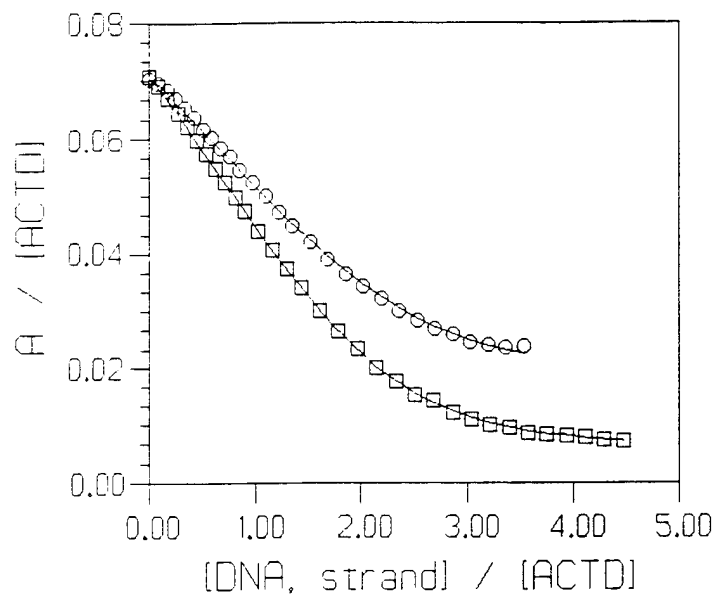


Figure 4

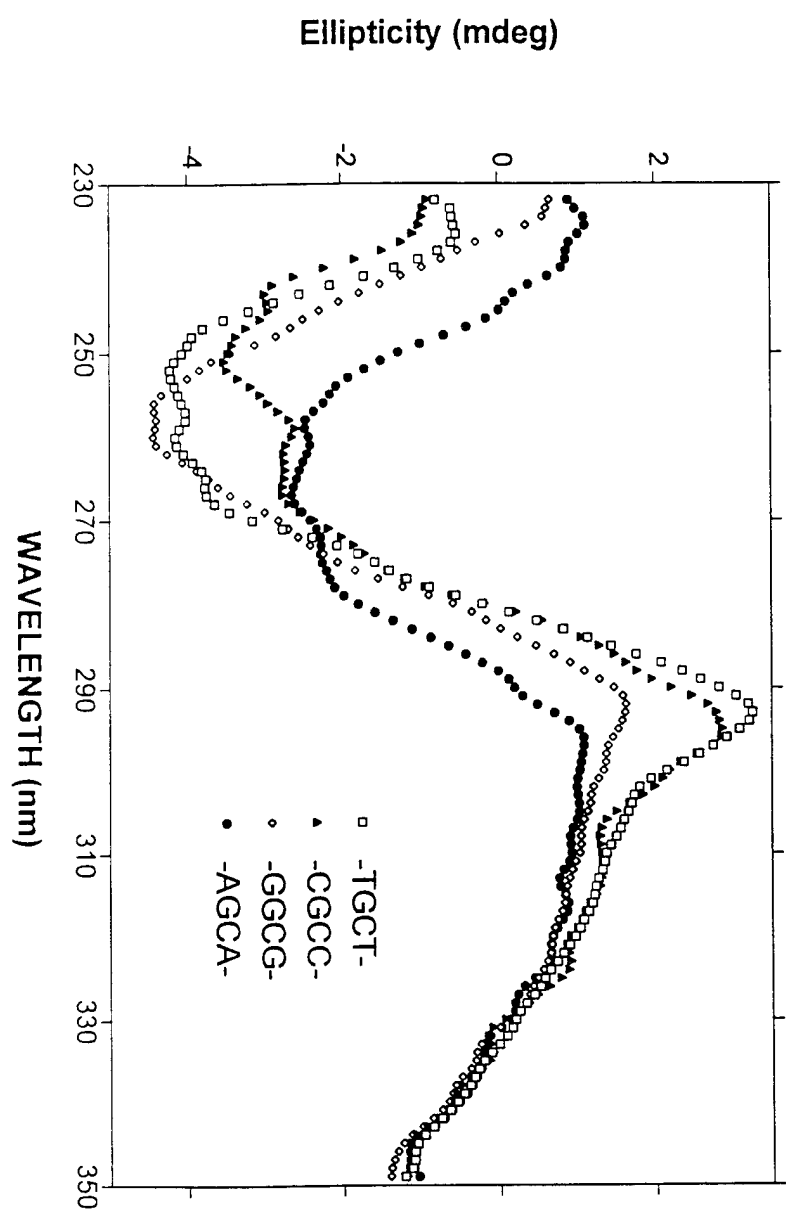


Figure 5

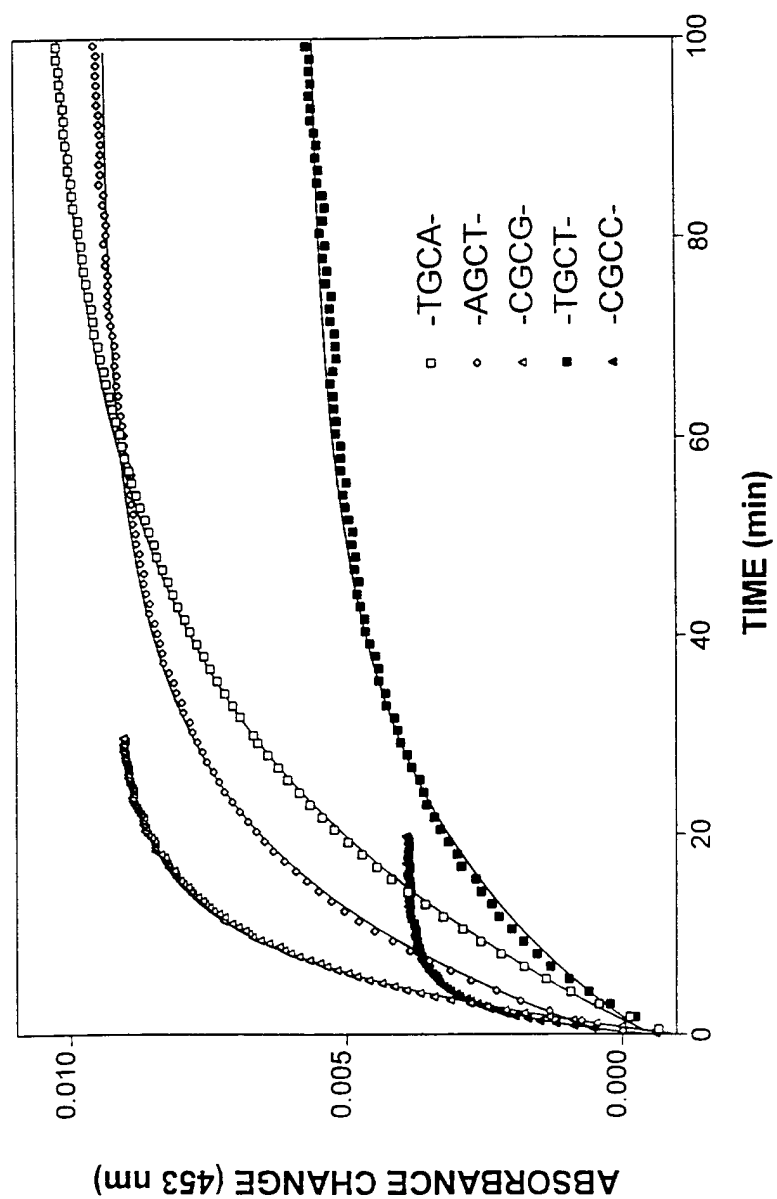


Figure 6

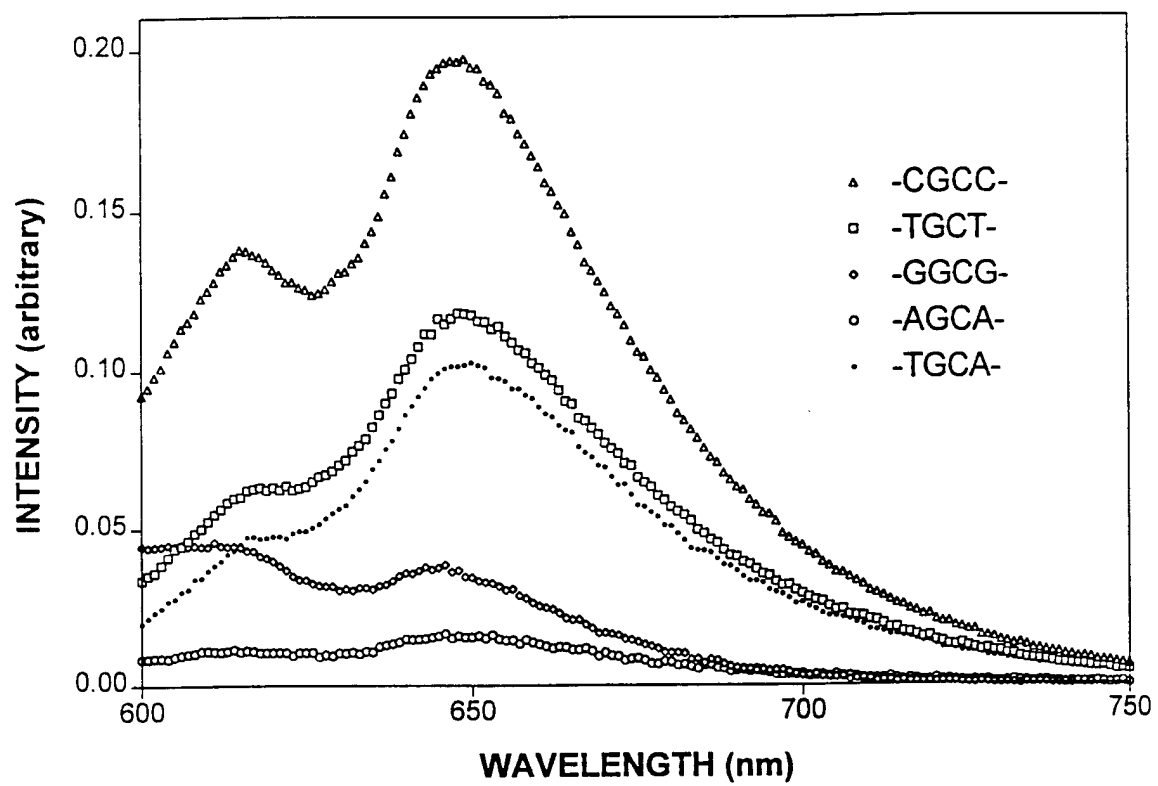


Figure 7

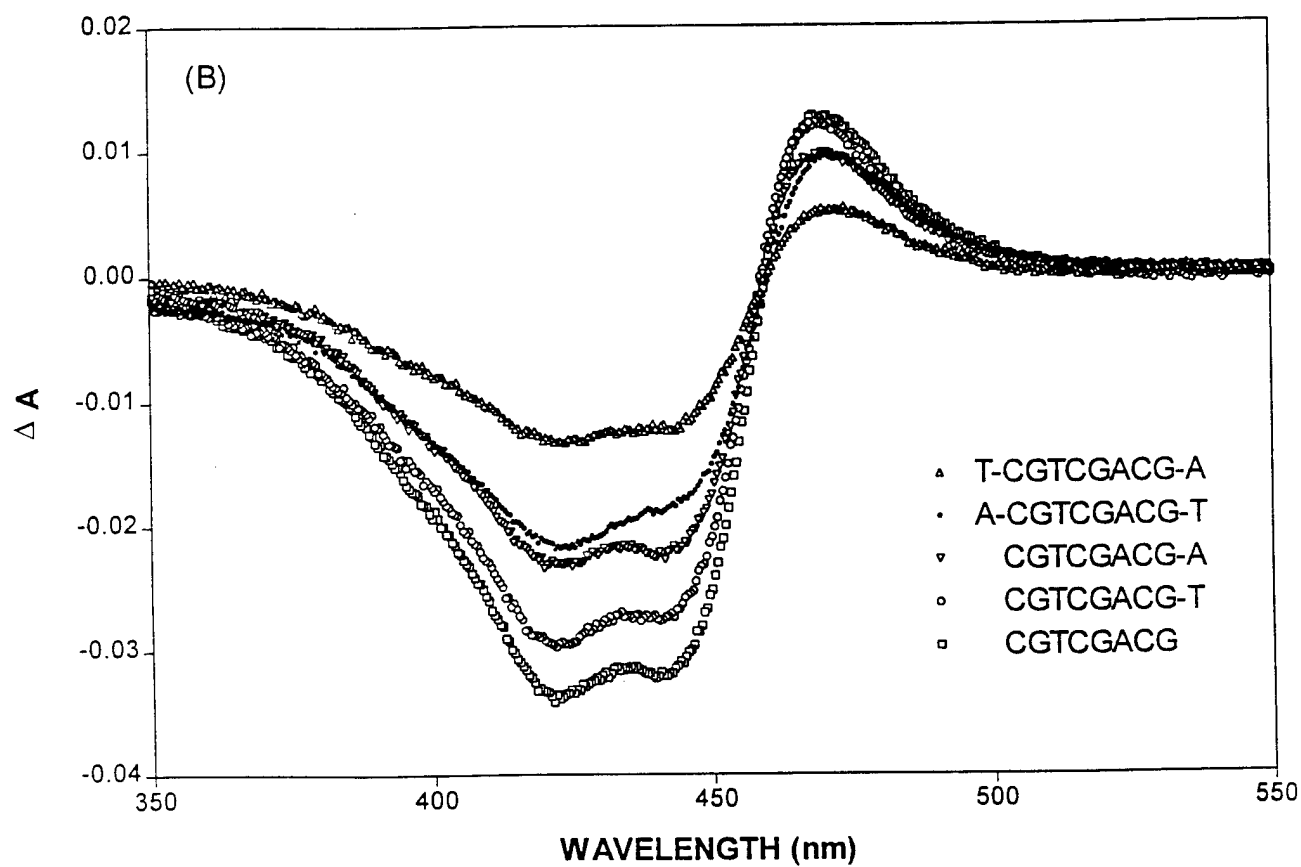
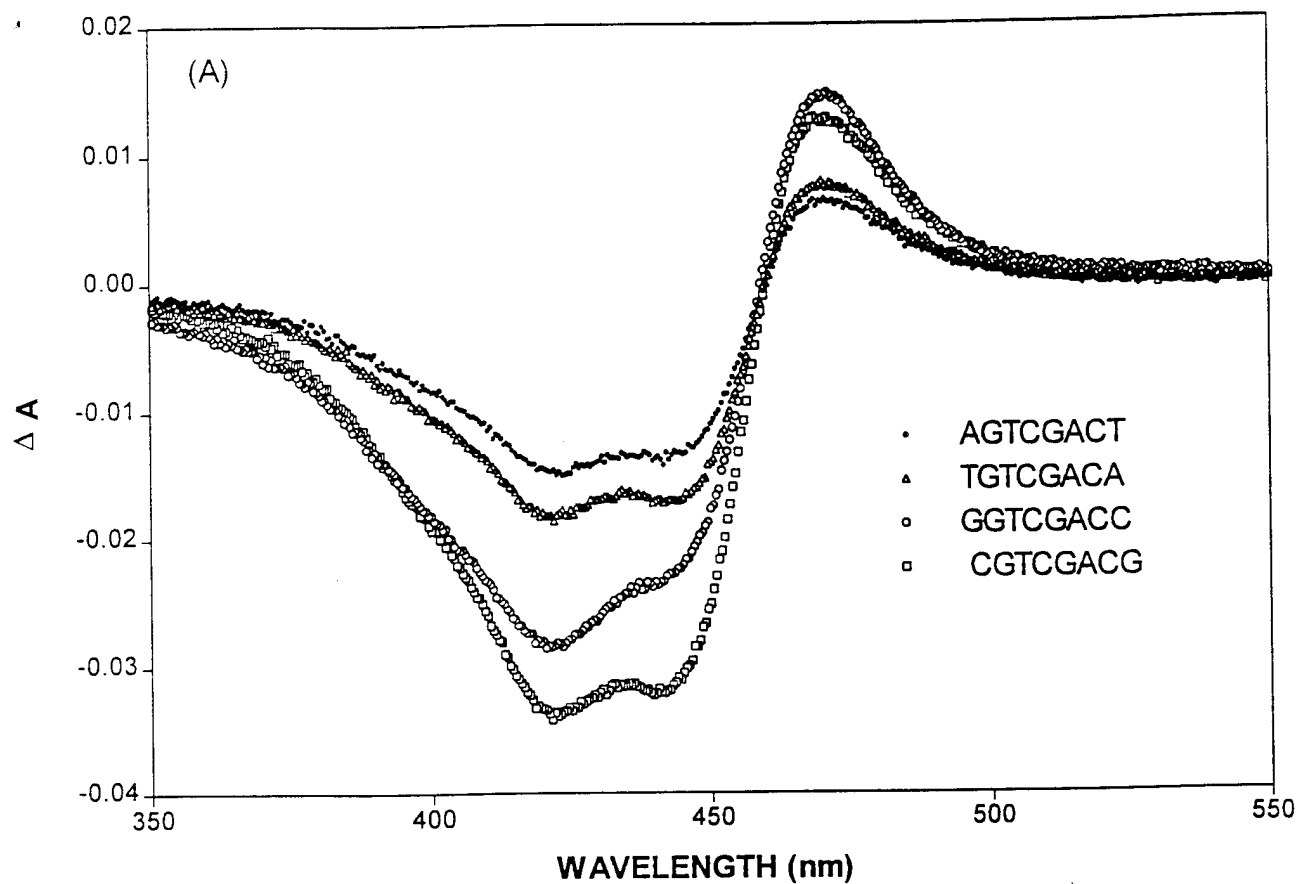


Figure 8

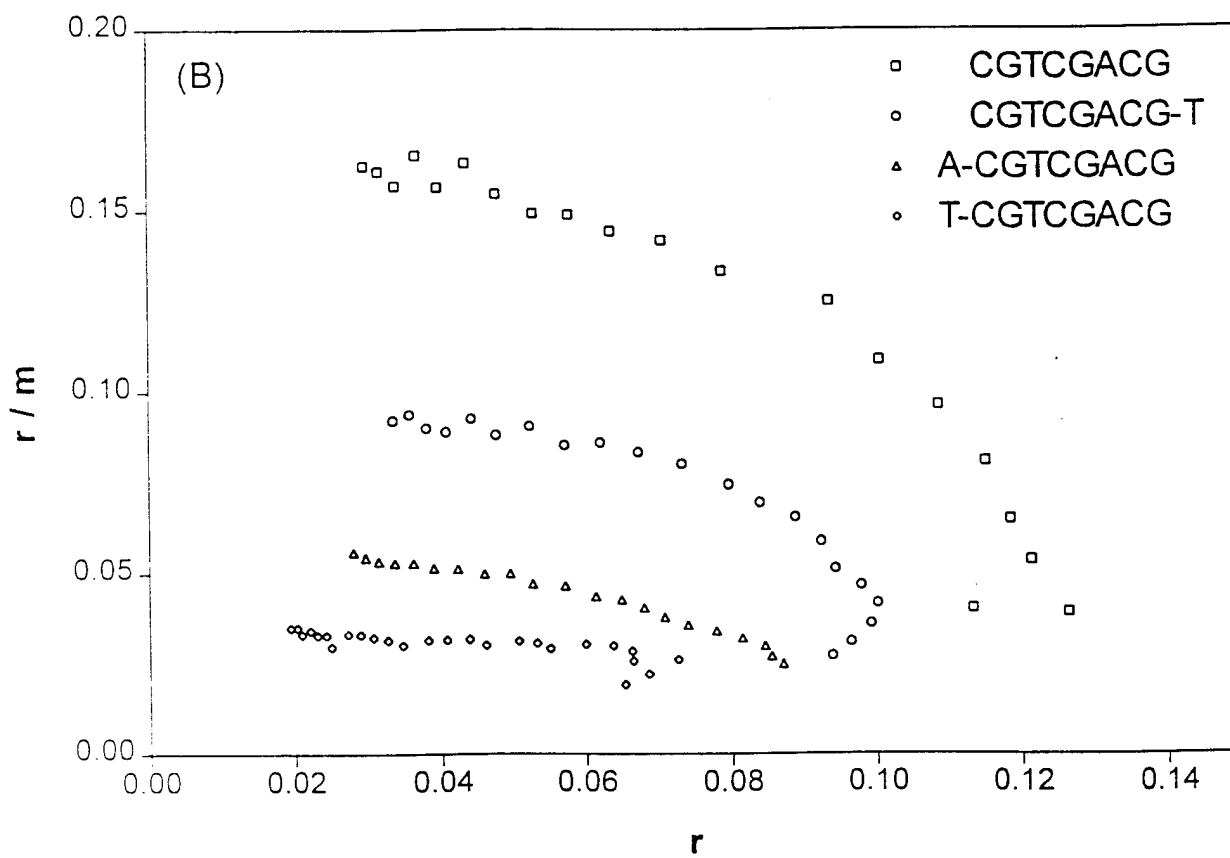
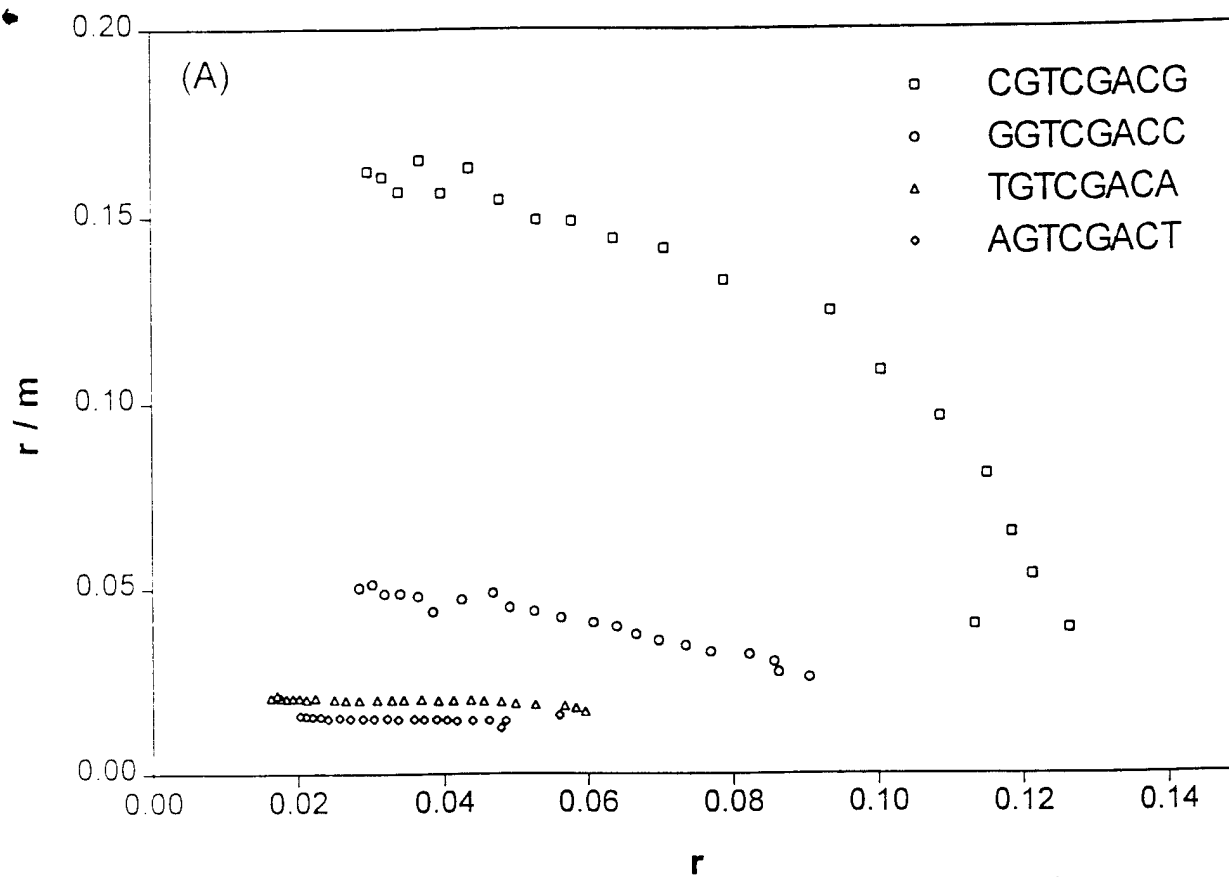


Figure 9

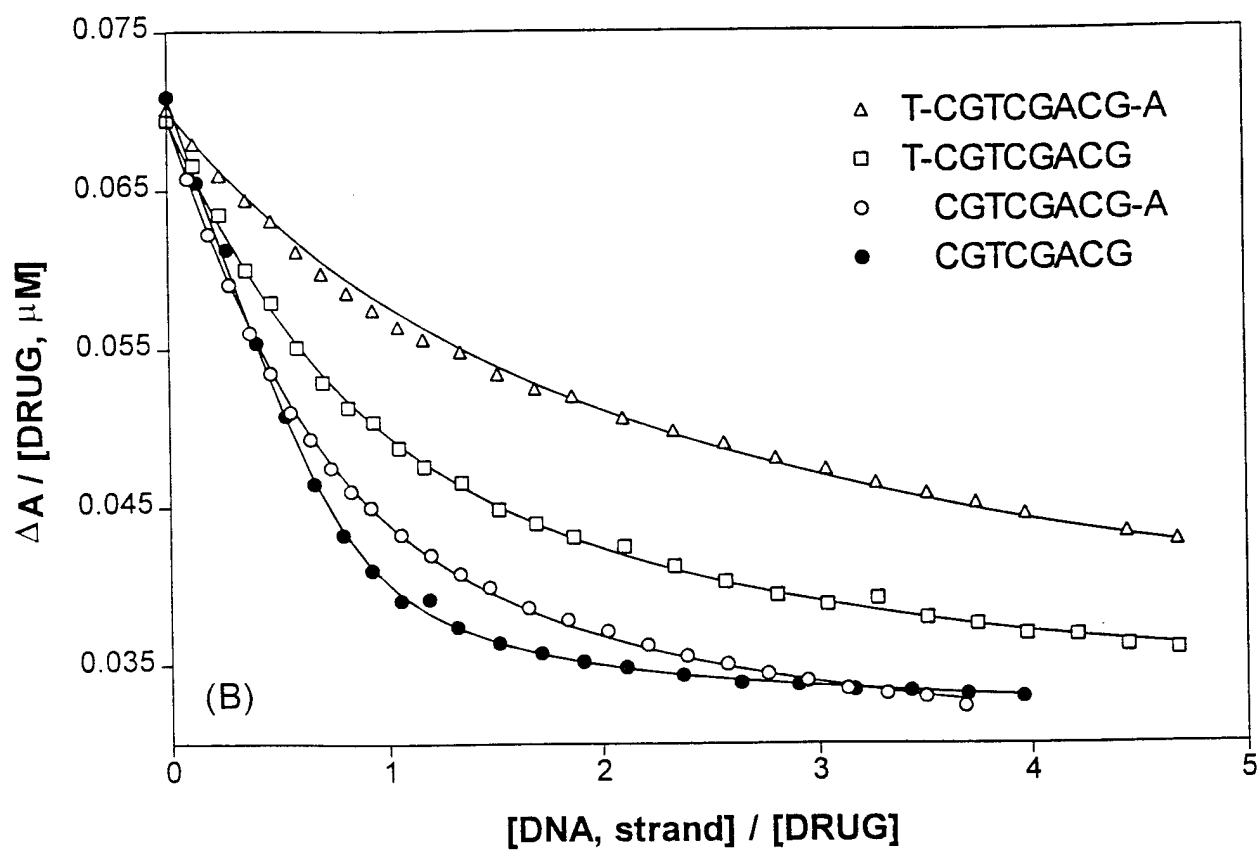
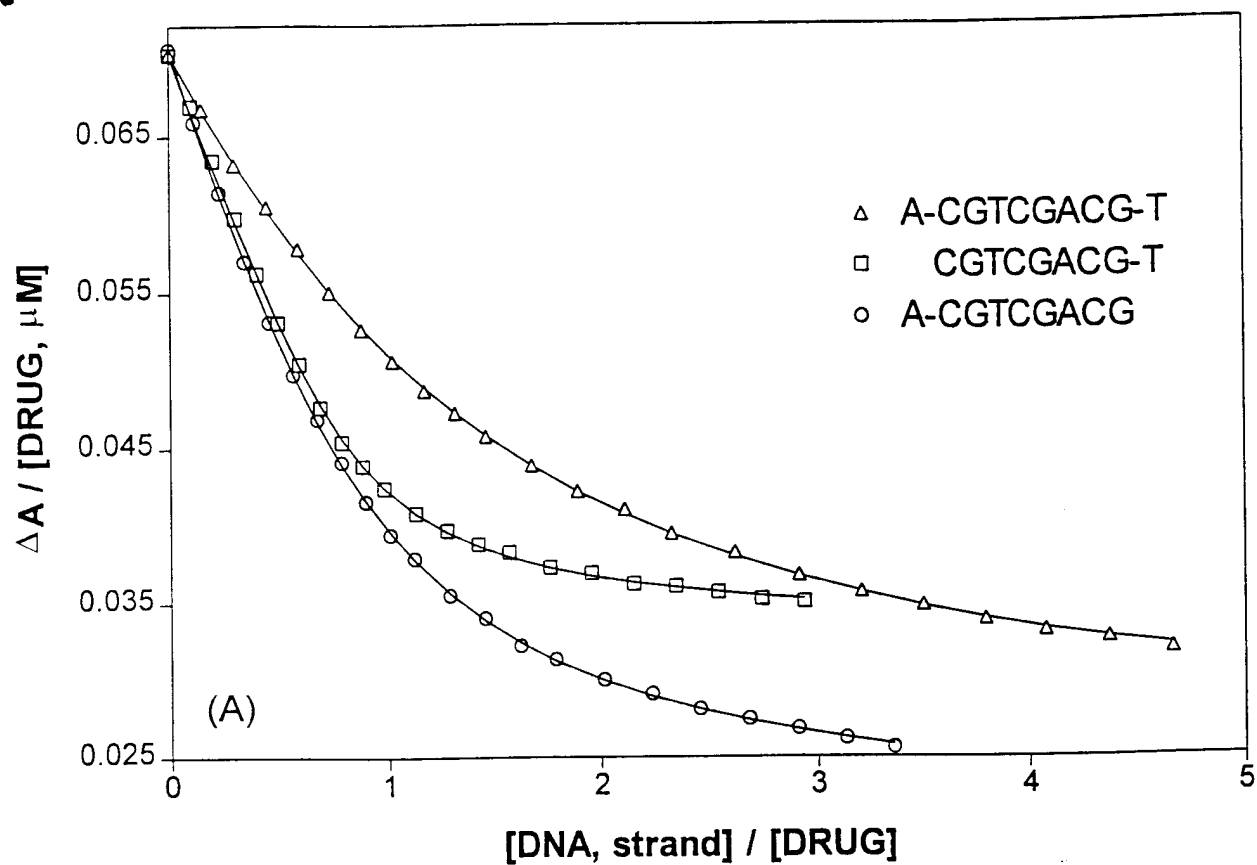
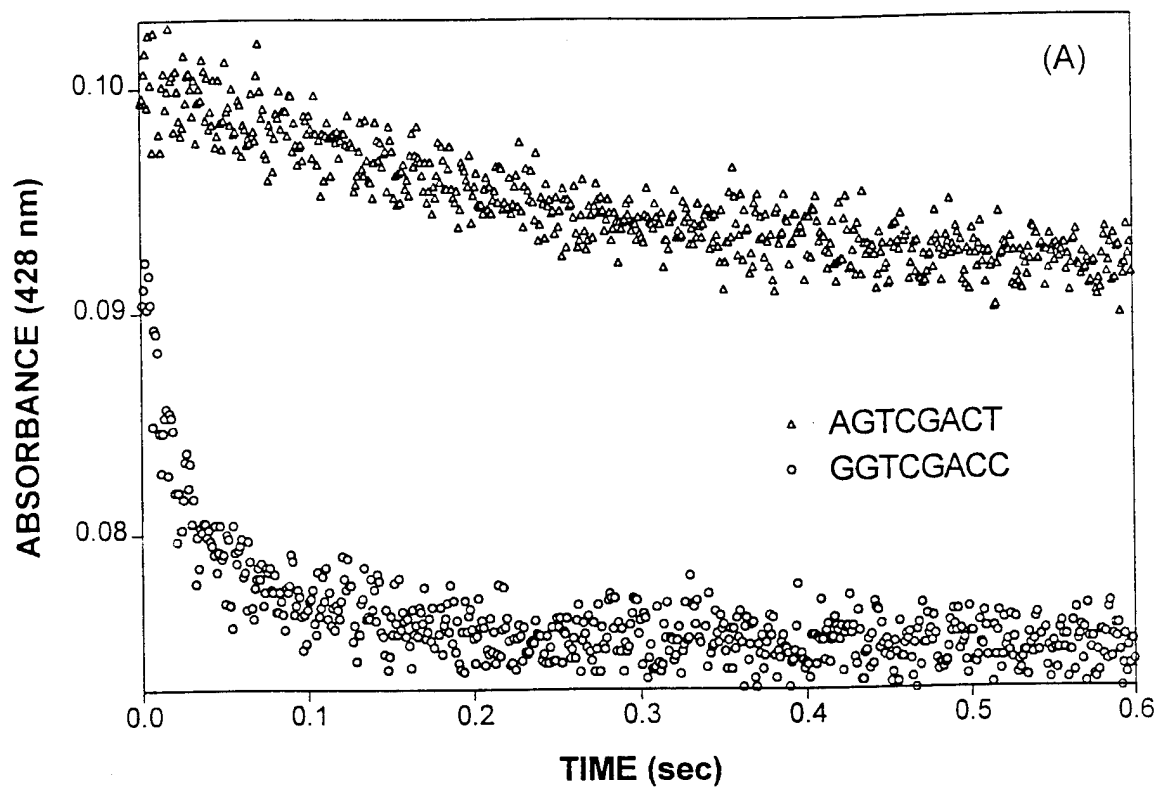


Figure 10 A



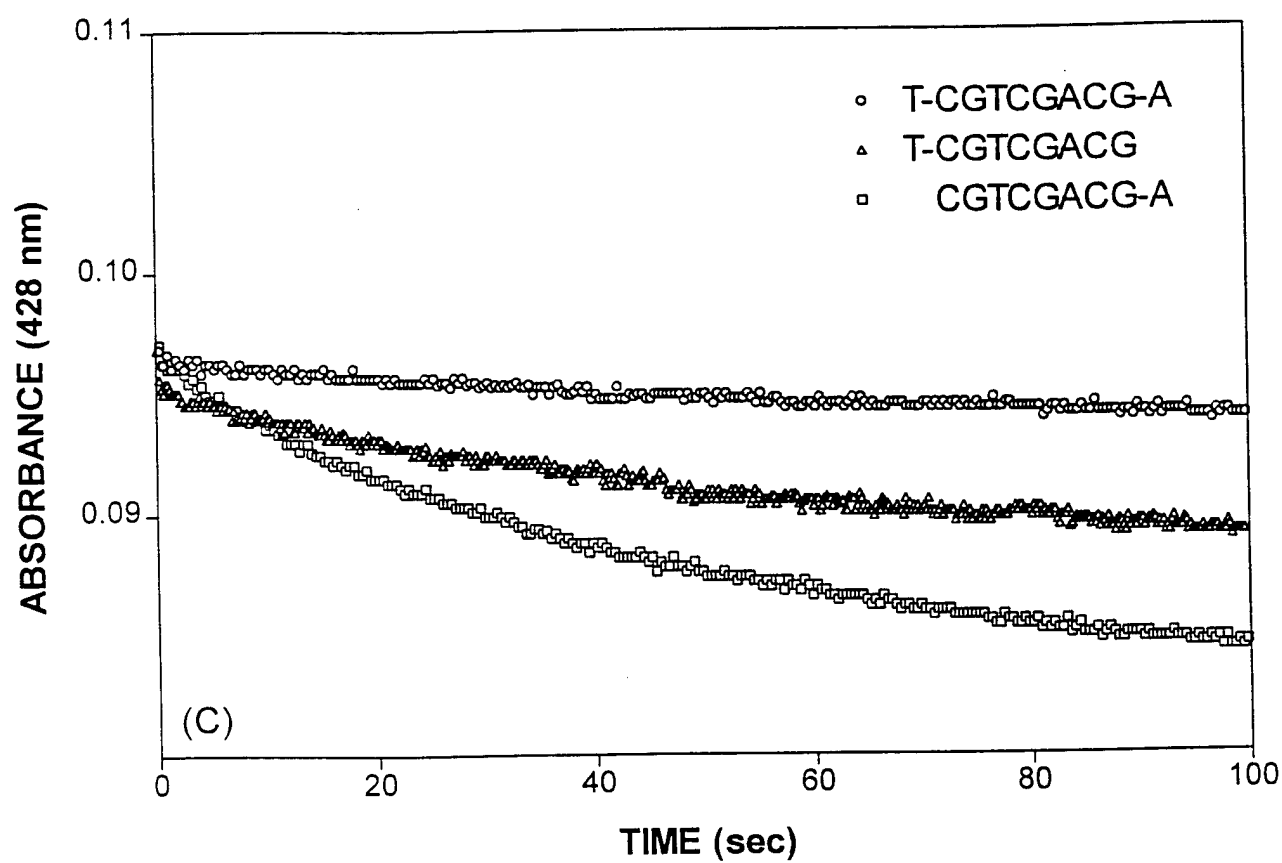
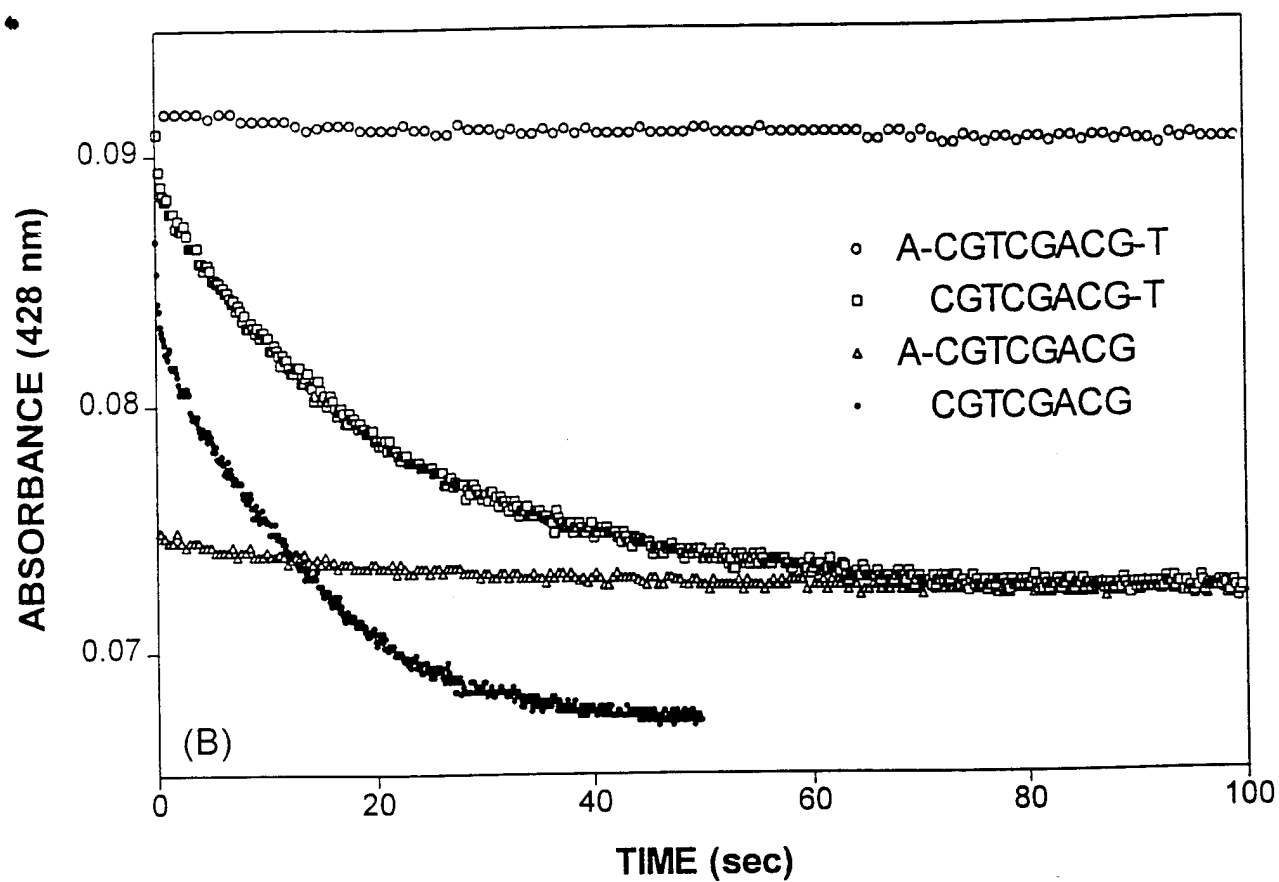


Figure 11 A

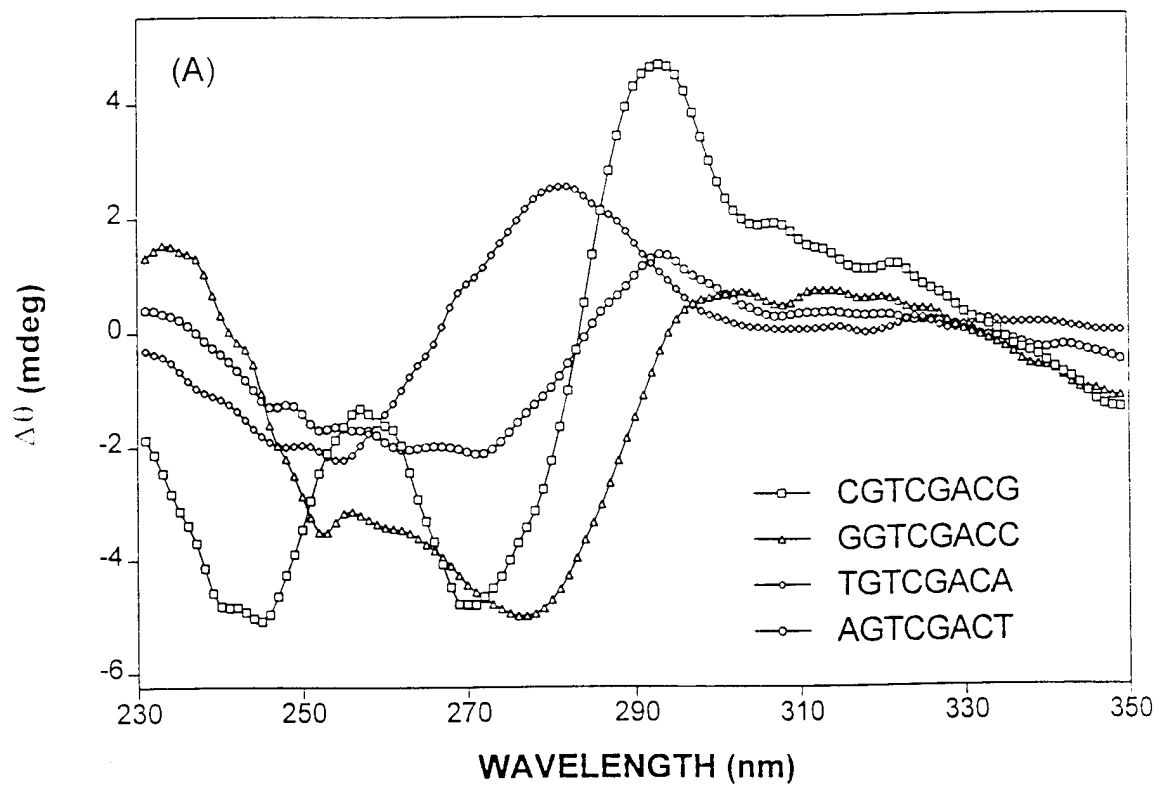


Figure 11 B,C

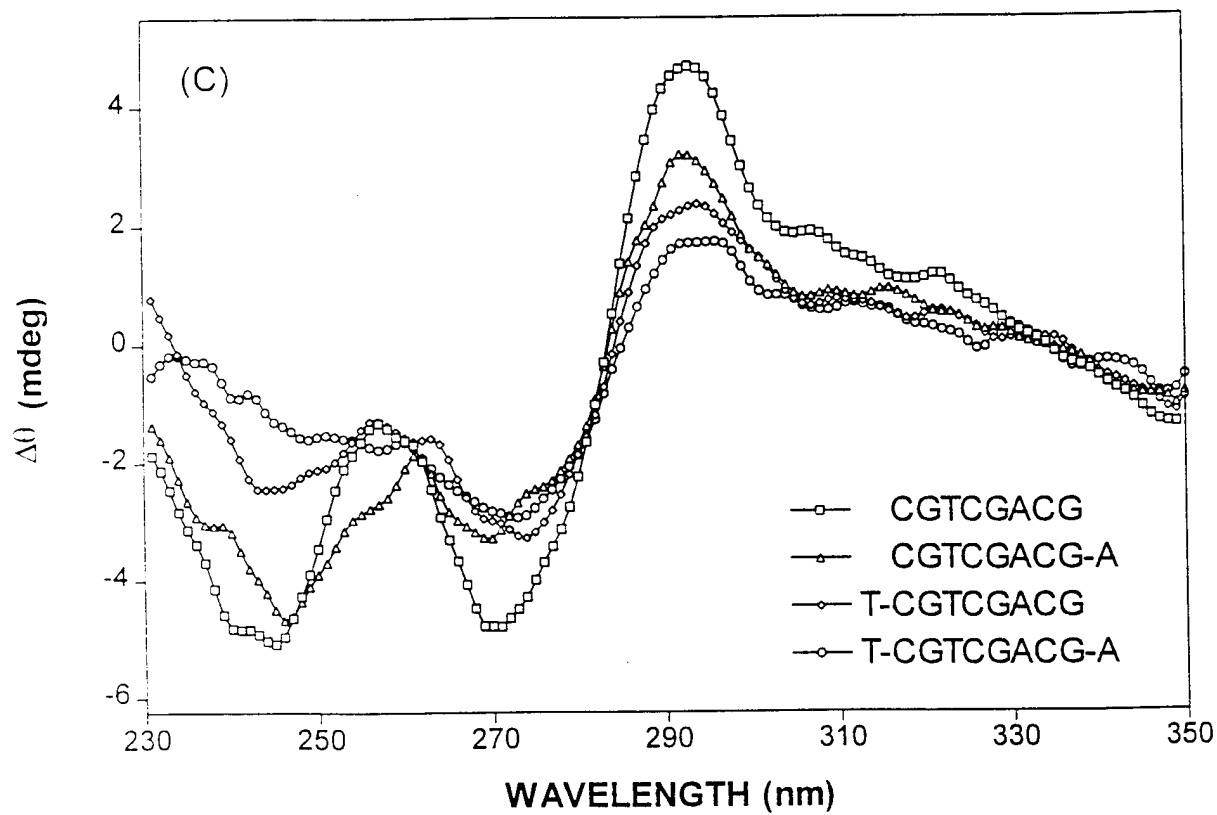
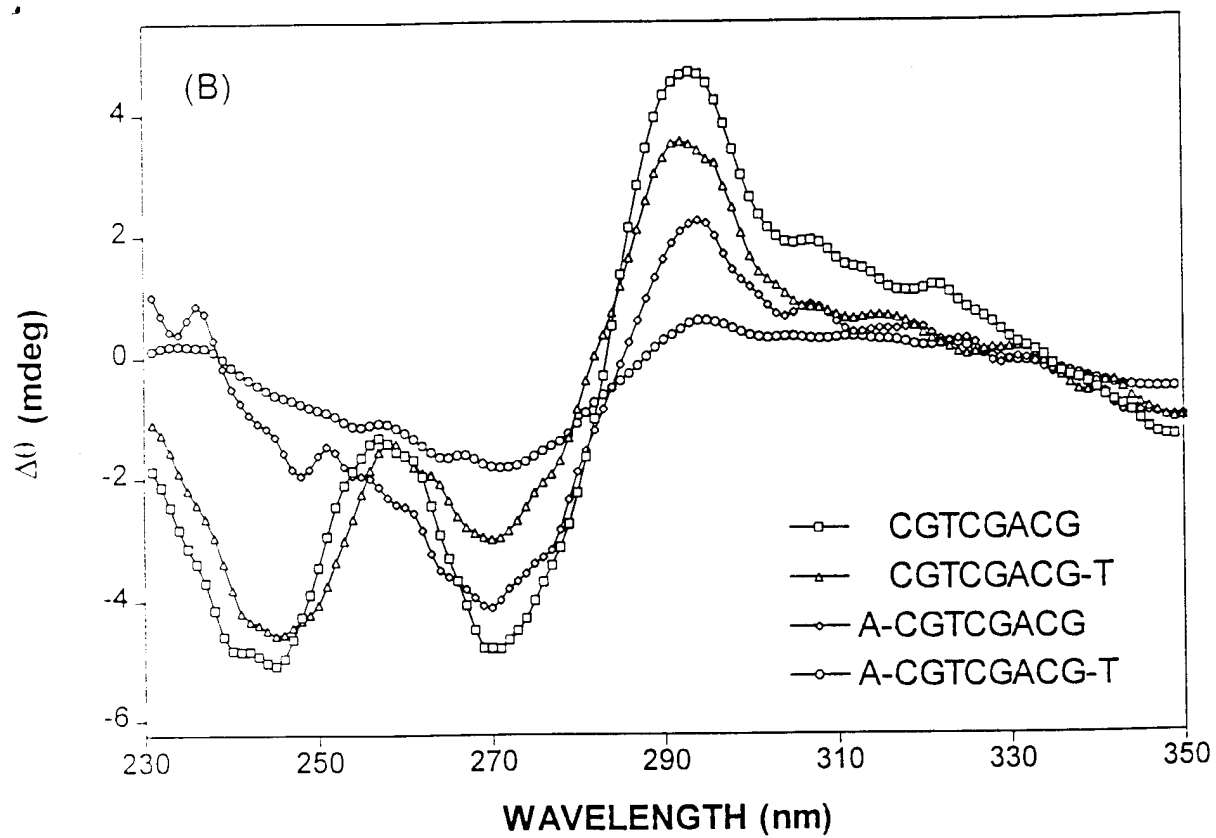


Figure 12

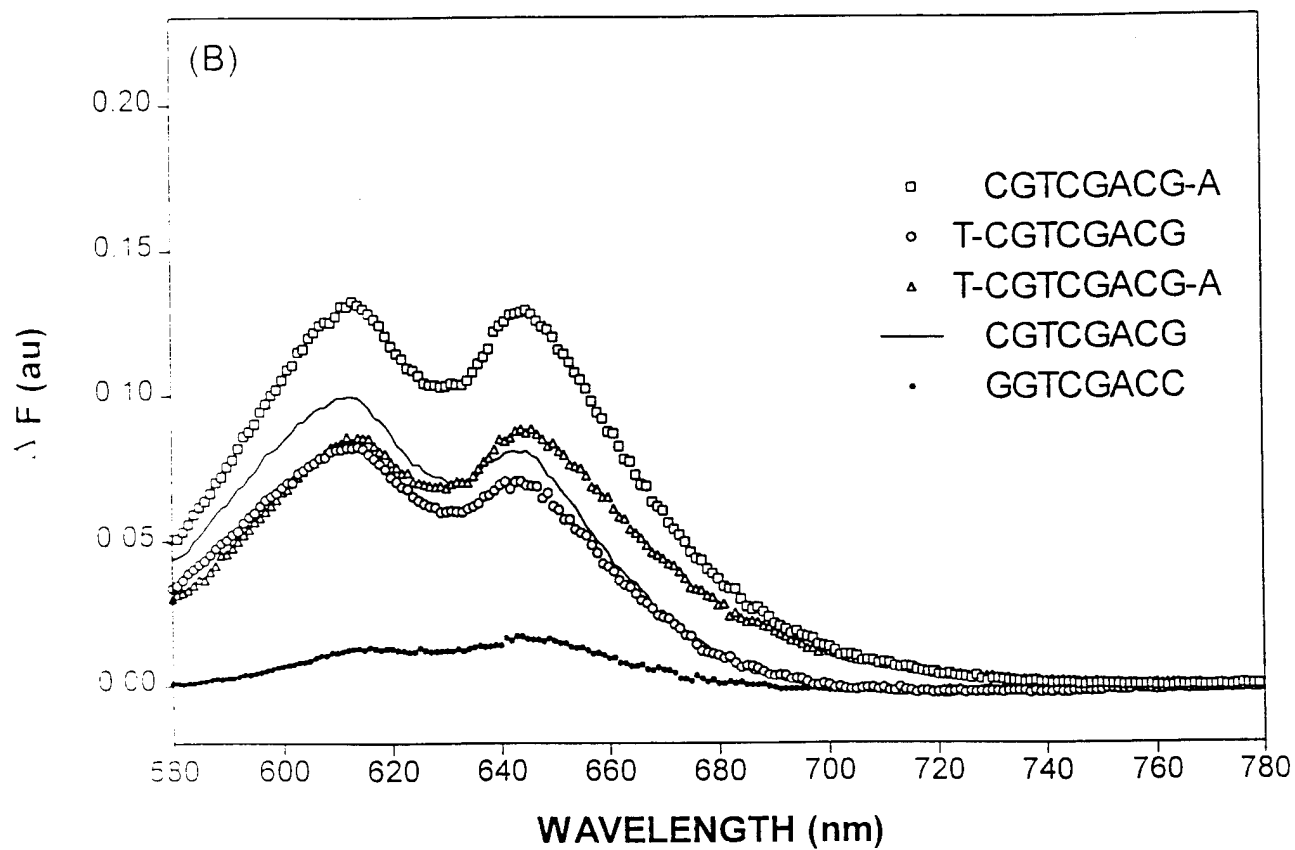
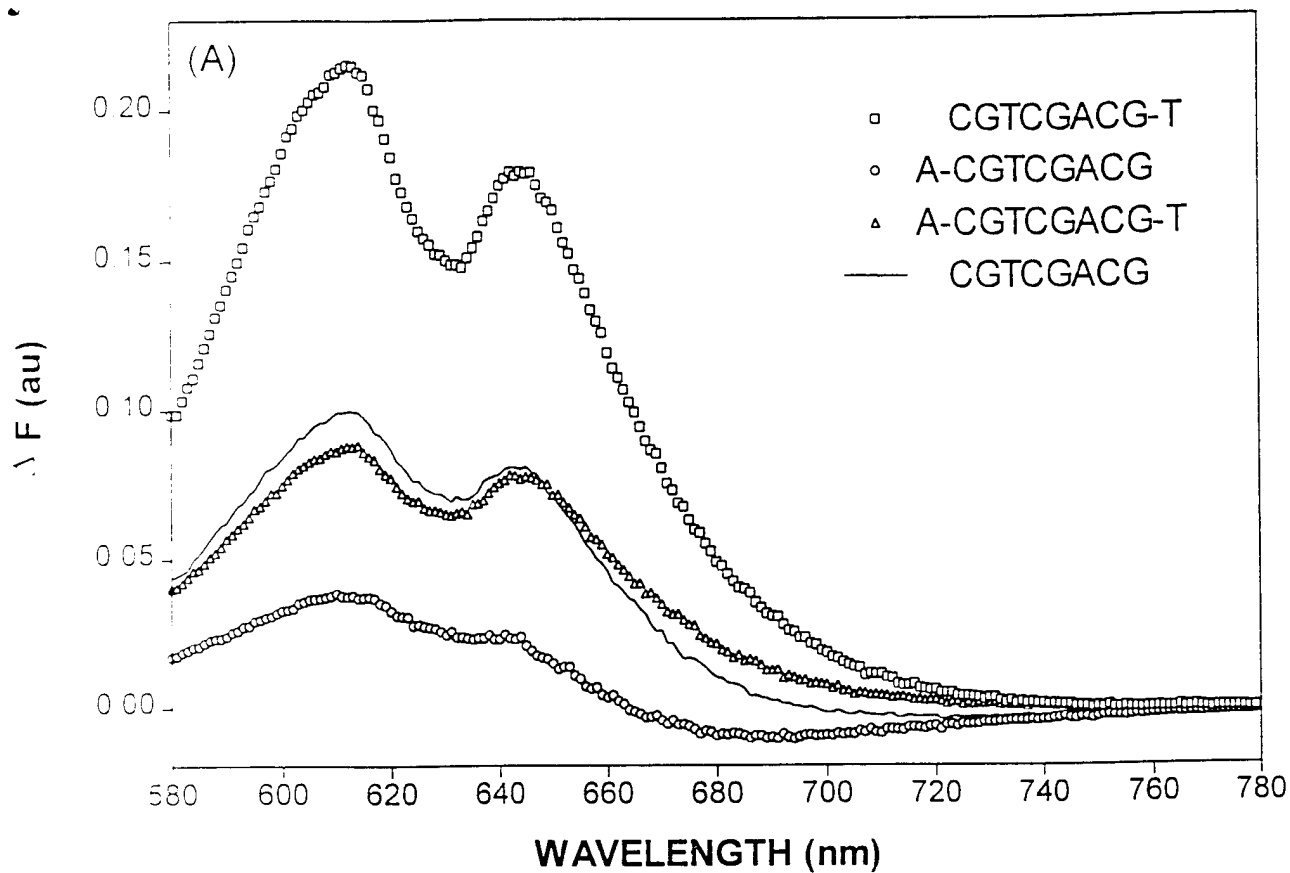


Figure 13

